

NSTAR Diagnostic Package Architecture and Deep Space One Spacecraft Event Detection

Michael D. Henry (Michael.D.Henry@jpl.nasa.gov)
David E. Brinza (David.E.Brinza@jpl.nasa.gov)
Anthony T. Mactutis (Anthony.T.Mactutis@jpl.nasa.gov)
Kenneth P. McCarty (Kenneth.P.Mccarty@jpl.nasa.gov)
Joel D. Rademacher (Joel.D.Rademacher@jpl.nasa.gov)
Thomas R. vanZandt (Tvanzandt@vaxeb.jpl.nasa.gov)

Jet Propulsion Laboratory
California Institute of Technology
4800 Oak Grove Drive
Pasadena, CA 91109-8099

Ron Johnson (Ron.Johnson@trw.com)
Stewart Moses (Stewart.Moses@trw.com)
TRW One Space Park
Redondo Beach, CA

Gunter Musmann (musmann@geophys.nat.tu-bs.de)
Institute for Geophysical and Meteorology
Technical University of Braunschweig
Braunschweig, Germany

Abstract—The Deep Space One mission is demonstrating the long-duration use of an Ion Propulsion Subsystem (IPS). The NASA Solar Electric Propulsion Technology Applications Readiness Project developed the NSTAR Diagnostics Package (NDP) to monitor the effects of the IPS on the spacecraft environment. The NDP measures contamination, plasma characteristics, electrical fields, and magnetic fields. This paper describes the NDP requirements, development process, and flight systems functionality.

NDP functionality exceeded expectations; it became an effective tool in the detection and diagnosis of spacecraft functionality and system anomalies. NDP detects hydrazine thruster firings (planned and not planned), ion engine gimbal stepper motor currents, solar array currents, spacecraft charging, as well as a number of other phenomena. Examples of selected ion engine and spacecraft signatures and their interpretations are discussed.

TABLE OF CONTENTS

1. INTRODUCTION
2. NSTAR DIAGNOSTIC PACKAGE REQUIREMENTS DEVELOPMENT
3. NDP HIGH LEVEL DESCRIPTION
4. FMP DESCRIPTION
5. RESULTS IN SPACE
6. CONCLUSION
7. REFERENCES
8. ACKNOWLEDGEMENTS

1. INTRODUCTION

NASA's New Millennium Deep Space One (DS1) mission is the first spacecraft to rely on solar electric propulsion (SEP) as the primary propulsion system. DS1 was launched on October 24, 1998. It successfully flew by asteroid 9969 Braille on July 28, 1999. It is currently on its way to comets Wilson-Harrington and Borrelly in 2001. The objective of DS1 is to demonstrate new technologies to be used on future missions. The 30cm diameter xenon ion propulsion system has been successfully validated as of the end of the primary mission. The engine is now being used as the main thruster to deliver the spacecraft to the two comets. For more information on the NSTAR projects see <http://nmp.jpl.nasa.gov/ds1/tech/sep.html>. For information on the DS1 mission and spacecraft see <http://nmp.jpl.nasa.gov/ds1/>. A brief description of the spacecraft can be found in [1]

For many years, ion propulsion has been considered a good substitute for chemical propulsion. Its thrust-to-weight ratio (specific impulse to weight ratio) is approximately ten times that of chemical propulsion. But mission managers have been reluctant to use it because of concerns about (1) cathode and grid wear, (2) possible spacecraft contamination from the engine, and (3) electromagnetic noise. The NASA SEP Technology Applications Readiness (NSTAR) Project set out to address the concerns by performing ground tests in vacuum chambers and by developing the Ion Propulsion System (IPS) to be demonstrated on the DS1 spacecraft. In order to validate the chamber measurements the NSTAR project developed the NSTAR Diagnostic Package (NDP). The NDP was developed and is being operated on DS1 to characterize the spacecraft IPS environment (see Figures 1 and 2). The NDP was designed to measure the contamination environment,

charge-exchange xenon plasma, plasma and electromagnetic noise, and magnetic fields generated by the ion propulsion system.

This paper discusses the top-level design of the NDP. It further describes the details of the Fields

Measurement Processor (FMP) and its associated sensors. Finally it discusses some preliminary results, including discussions of unexpected phenomena observed by the NDP.

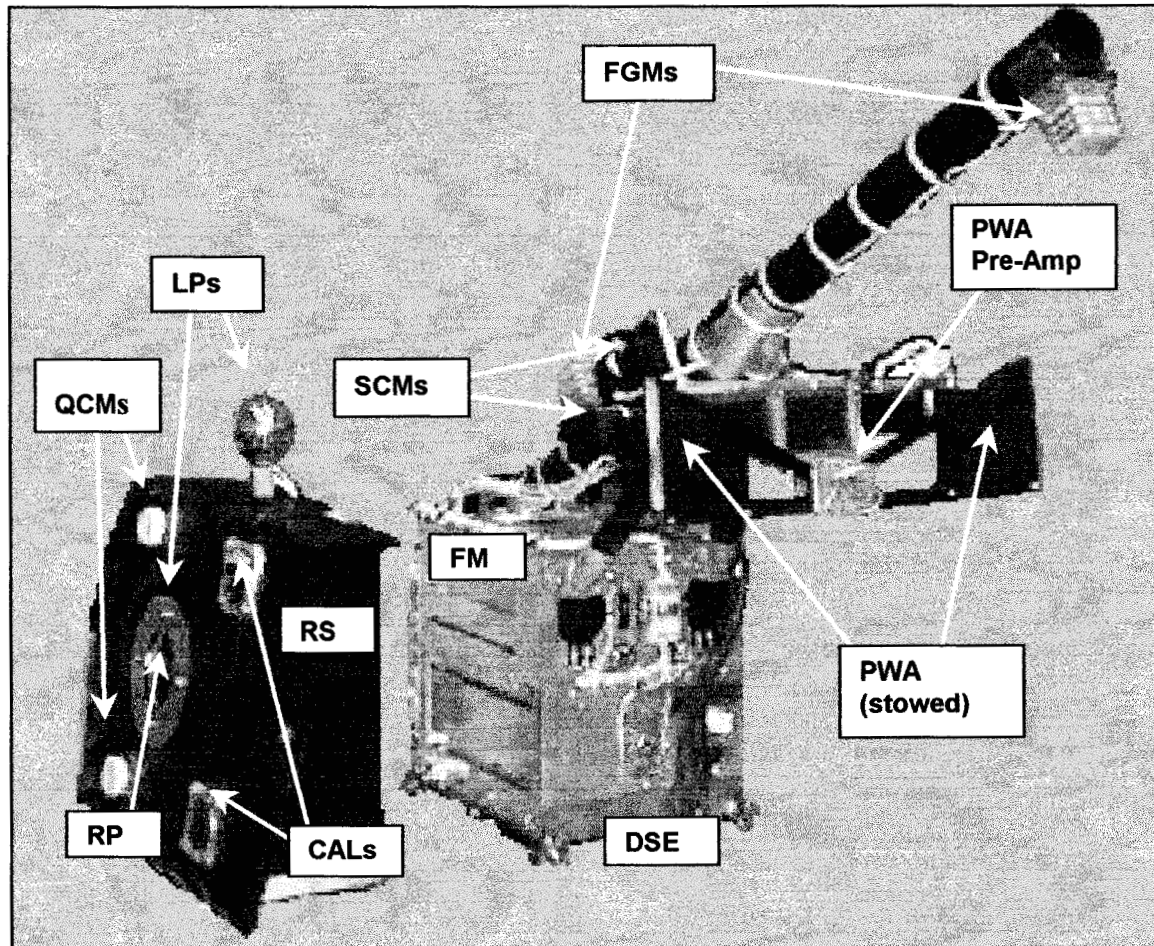


Figure 1. NSTAR Diagnostics Package by Itself

2. NSTAR DIAGNOSTIC PACKAGE REQUIREMENTS DEVELOPMENT

For many years mission planners have considered ion propulsion as being an enhancing, and in some cases, enabling technology. But concerns about effects of the ion propulsion on the spacecraft and instruments have hampered its acceptance. To help alleviate these concerns, workshops were held and surveys were made to identify the concerns and determine means of validating ion propulsion to make the technology viable [2],[3],[4].

The consensus of the workshop participants was that the most important high-level validation requirements were the following:

- Identify surface contamination from eroded grid material
- Determine erosion of spacecraft surfaces from energetic charge exchange ions
- Measure plasma density and plasma effects on power system and science instruments

- Identify electron temperature and spacecraft potential charging
- Measure engine-produced electromagnetic interference (EMI) and its effects on instruments and spacecraft subsystems
- Measure DC and AC magnetic fields
- Measure plume effects on spacecraft communications

Along with the concerns of the potential destructive effects of the ion propulsion system, issues of SEP effects on science instruments operation were identified. The major evaluation requirements follow:

- Identify the effect on particles and fields instruments operating during thrusting
- Identify plasma/plume instabilities and their interactions with the solar wind

Many ground tests were performed to measure the ion propulsion characteristics that could affect spacecraft systems and instruments. Although, chamber tests are important, they fall short of providing a true space environment. Also, as space measurements were made, it became clear that spacecraft systems were as noisy as the

ion propulsion system and that our measurement schemes should have been different in some cases to

get more of the desired data.

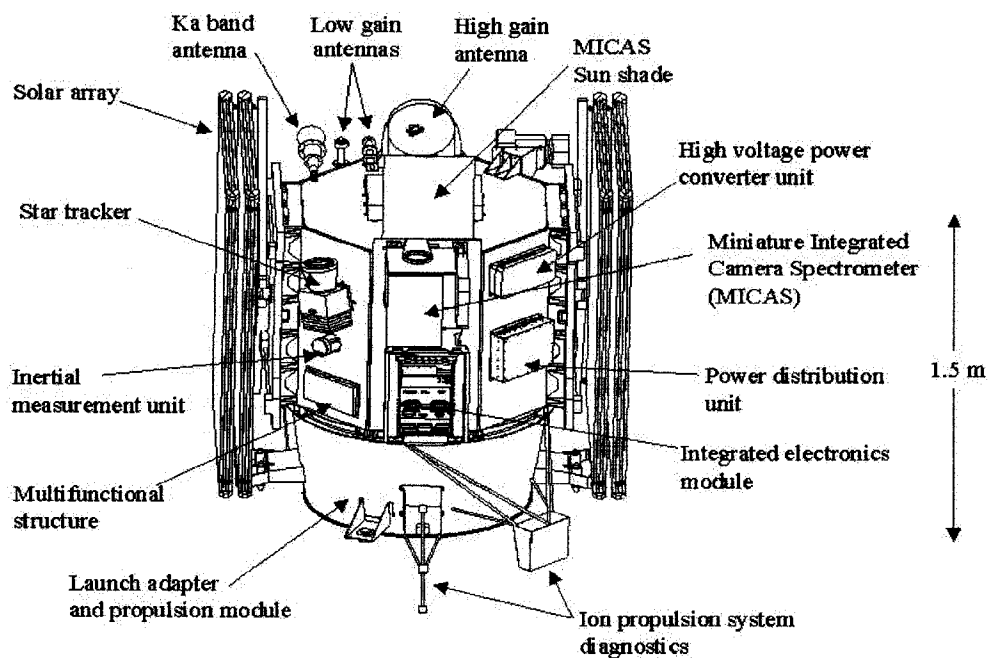
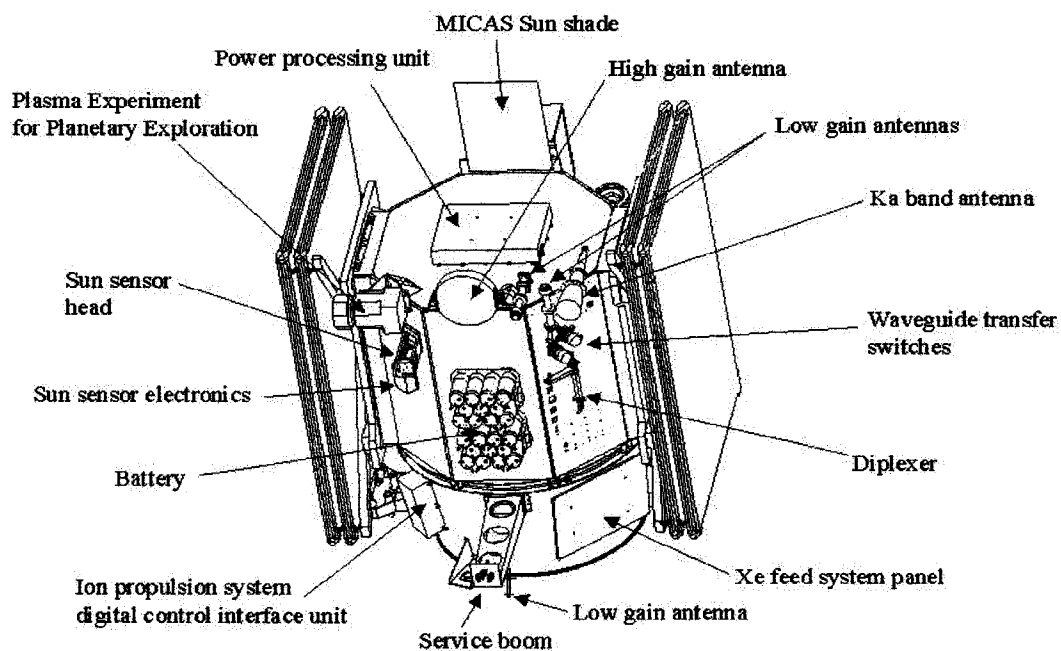


Figure 2. NSTAR Diagnostics Package on Deep Space 1 Spacecraft

Result From Ground Test

As part of the NSTAR ground test program, the NDP task developed fields sensors similar to those being planned for the flight mission. Passive and active monopole antennas were installed in the chamber for testing during the 8000-hr test and the CT31 and CT36 tests. Passive and active search coils were also used during these tests.

Data analysis showed that the ion engine produced a worst-case spectrum of 0.1 V/m from DC to 20 MHz and was bounded by 0.001 V/m from 20 MHz to at least 60 MHz for the PWA and SC0. Also the engine recycles and engine startups produce transients in the time domain of less than 10 V/m for both the PWA and the SC0.

During the tests, we noticed that the broad channel spectral data did not show the character of the engines state as did the time domain data. Data and test methodology from previous test performed at the John H. Glenn Research Center (formerly Lewis Research Center) were compared to our results and methods.

In order to determine the magnetic field measurement requirements, we magnetically mapped the engineering model thruster.

NDP Requirements

As with most projects, other factors influenced the design of a system. The funding available for the NDP development originally did not allow for much in the way of fields measurements. Creative negotiations with some members of the fields and particles science community resulted in a teaming effort of TRW, Technical University of Braunschweig (TUB), and the JPL Integrated Space Physics Instrument (ISPI) project. TRW agreed to provide the Plasma Wave Pre-amp and Spectrometer board. TUB agreed to provide two sets of three-axis flux gate magnetometers and signal processing board. ISPI provided support for the development of the engineering search coil. The ISPI project also provided the science search coil.

Results of the ground tests combined with capabilities of the donating organizations resulted in the following capabilities of the flight system.

Search Coil Magnetometer

- Single-axis measurement
- Amplitude 1 nT to 0.1 mT
- 10 Hz to 30 kHz

Plasma Wave Spectrometer

- Effective Length Dipole Antenna: 1 m
- Amplitude: 1 μ V/m to 10 V/m
- Spectral Frequency Range: 10 to 50 MHz
- Four bands (channels) per decade
- Time domain signals: 20,000 samples/s sample rate.

Flux Gate Magnetometer

- Two, three-axis sensors
- Full-scale range: ± 5000 nT

- Sensitivity: ± 0.1 nT
- Sample rate: 20 Hz

Transient Time Domain Capture

- Simultaneous record time domain samples of plasma wave, search coil and magnetometer data
- A 1-s set of 20,000 samples/s plasma wave data
- A 1-s set of 20,000 samples/s search coil data
- A 1-s set of 20 samples/s magnetometer data (six channels)

Transient Detection

- Sample time domain to meet the above transient time domain capture data while performing scan data recording
- Detect large signal peaks for both search coil and plasma wave
- Record data prior to and after event detection

3. NDP HIGH LEVEL DESCRIPTION

As shown in the block diagram of Figure 3, the NDP consists of twelve sensors, sensor conditioning circuitry, and two micro-computers to collect and process the data. The NDP package is functionally separated into two subsystems, the Diagnostic Sensors Electronics Unit (DSEU) and the Fields Measurement Processor (FMP). The DSEU sensor suite consists of two quartz crystal microbalances (QCM), two optical solar reflector calorimeters, two Langmuir probes, and one Retarding Potential Analyzer (RPA). The FMP sensor suite consists of a 1-meter dipole Plasma Wave Antenna (PWA) and pre-amplifier, a single-axis flux balancing miniaturized search coil (SC0), a science search coil (SC1), and a pair of tri-axial flux gate magnetometers (FGM 0 & 1).

The science search coil SC1's pre-amp was damaged by large stray magnetic fields on the launch pad. Because SC1 is not functional, it is not addressed in this paper.

The DSEU communicates with the spacecraft and the FMP. The DSEU performs signal conditioning and data formatting for the QCMs, the calorimeters, the Langmuir probes, and RPA. The DSEU samples the sensor data once every two seconds and provides the data to the spacecraft in specific Mil-Std-1553 subaddresses. The DSEU receives spacecraft time and keeps a running clock to time-tag the data. The DSEU periodically receives data from the FMP via an RS-232 bidirectional serial port. The FMP performs signal conditioning and signal processing for the PWA, SC0, and FGM's.

The FMP collects FGM data from the FGM electronics package. The FMP collects two types of PWA and SC0 data. Every 16 seconds the FMP collects scan spectrometer data and sporadically provides "Burst" time domain data. The PWA scan data is spectral data over six and a half decades, 10 Hz–40 MHz, four bands (aka channels) per decade. The SC0 scan data is spectral data over four decades, 10 Hz–100 kHz, four bands per decade. The PWA/SC0 Burst data is 20,000 samples of time domain data collected at 20,000 samples a second. The scan FGM data is sixteen sets of data. Each set is the average of 20 samples, in a one-second interval. The Burst FGM data is a collection of the FGM data sampled at 20 samples a second, for one second.

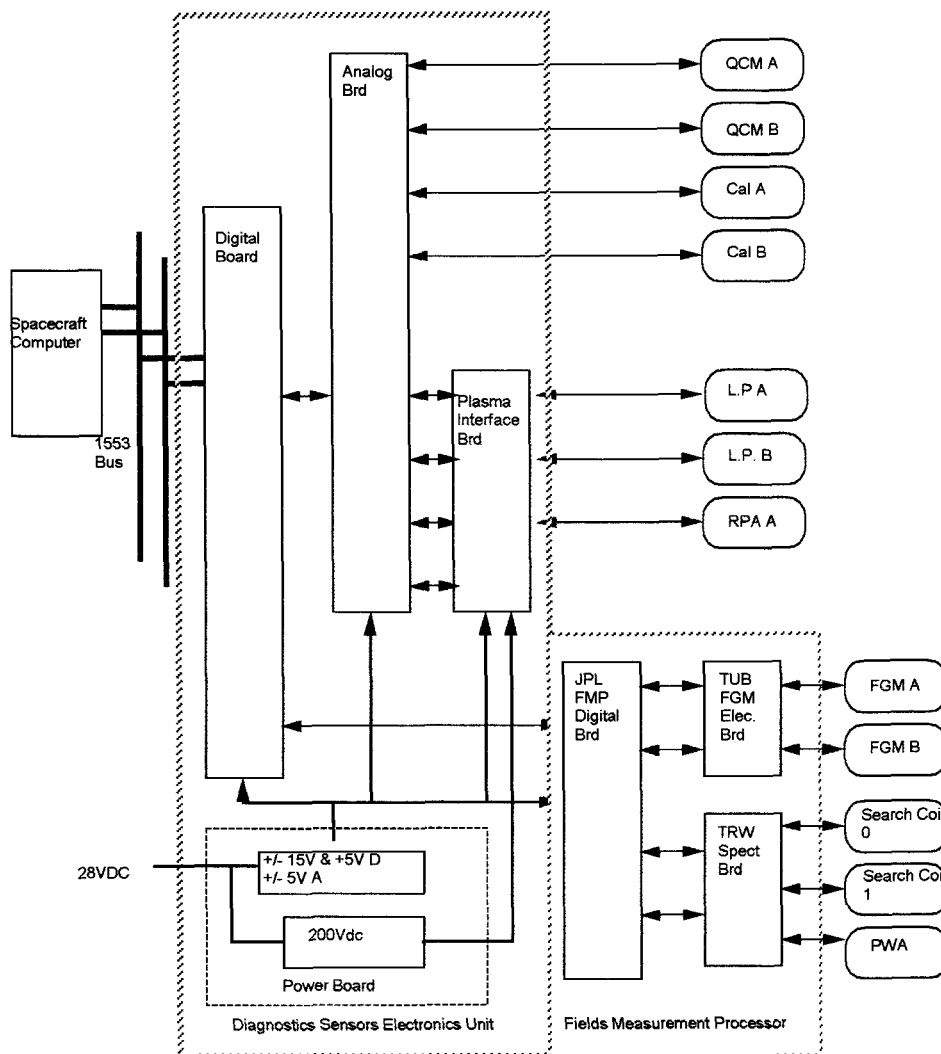


Figure 3. NSTAR Diagnostic Package Block Diagram

4. FMP DESCRIPTION

The FMP (Figure 4) consists of an FMP digital board, a spectrometer board, an FGM signal conditioner board, and the sensors. The FMP electronics are housed in a chassis, which mounts on top of the DSEU chassis. An external harness provides the interconnection between the FMP boards and the DSEU. The DSEU provides the conditioned power to run the FMP. The FMP is switched on and off by the DSEU.

The FMP was developed with a highly constrained budget. The FGM's and their electronics were developed and contributed by TUB. TRW developed the PWA pre-amp and Spectrometer board with Internal Research and Development funds. The funding for the JPL FMP Digital board was a small fraction of the NSTAR contingency funds. All the FMP avionics boards have some commercial parts. At least half of all the parts in the FMP are plastic packaged. Many of the parts were leftovers of different previous projects, which we were able to get for free.

Creative design practices were used to develop the FMP digital board to make it radiation tolerant. The FMP digital board's digital signal processor (DSP) is latch-up prone and susceptible to single event upset (SEU). The program store FLASHROM is suspected to be a 1-2 kRad part. The FMP digital board designer developed a creative design utilizing a radiation-hard gate array and a current-sensing circuit to monitor the radiation-soft circuits. If the DSP latches up, the current-sensing circuit detects a large current rise, and the gate array shuts off the power to the DSP. Then the gate array powers the total-dose-sensitive FLASHROM device and the DSP to load the DSP's instruction code. Then the gate array powers off the FLASHROM. This approach utilized the little known fact that most electronics are not changed by total dose when they are powered off. Since the FLASHROM has only been switched on for a couple seconds over the whole mission, there has been no observed degradation in the part due to radiation total dose.

Though there were requirements from the studies and conferences, the FMP capabilities were largely constrained and directed by capabilities and available resources. Schedule, budget, and resources over ruled desirabilities and requirements.

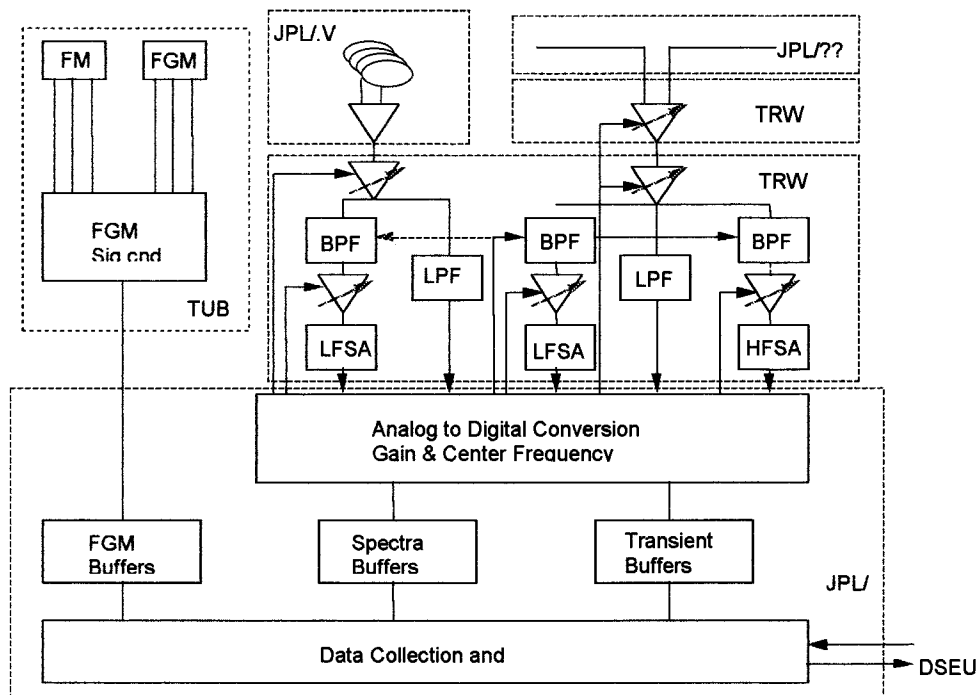


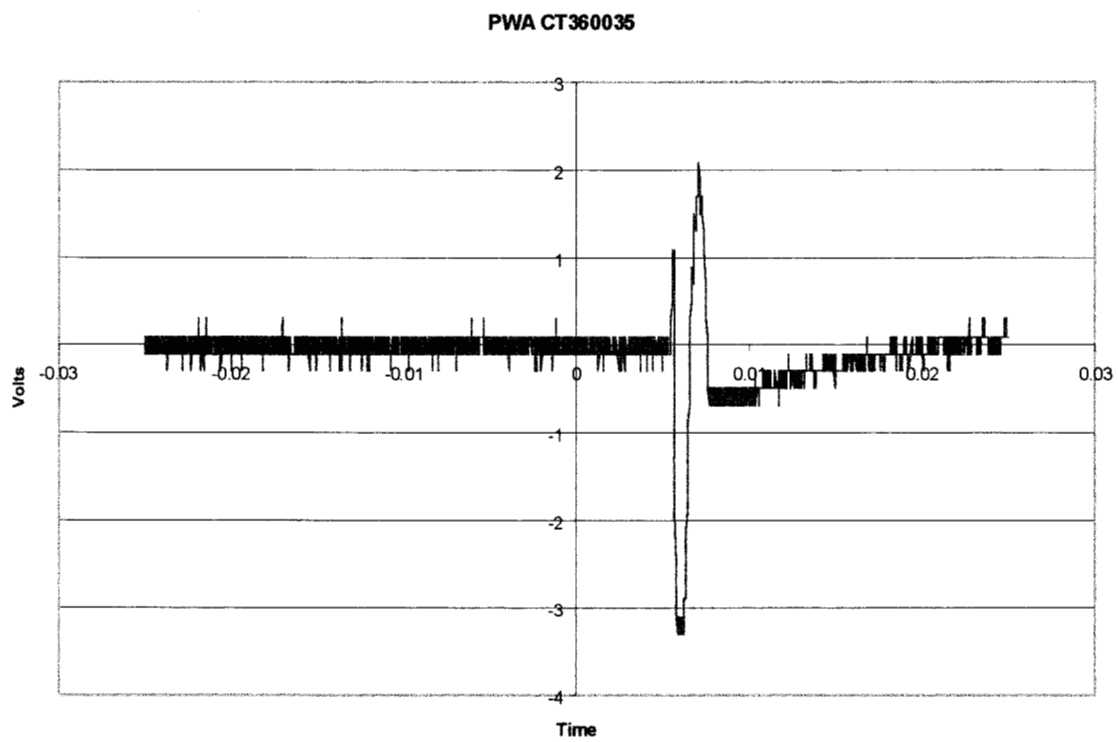
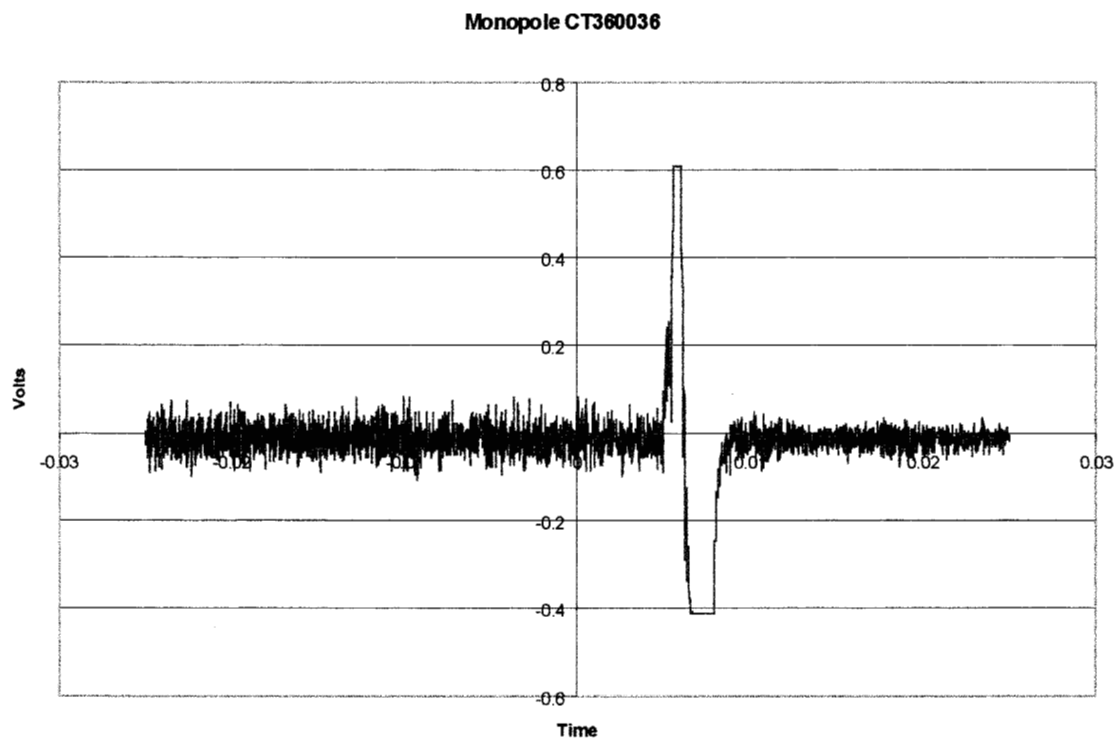
Figure 4. FMP Block Diagram

The FMP provides two major functions, it collects "scan" data on a 16-second period. And it has a time domain collection capability. The scan processing is always active. The data is collected, processed, packaged, and sent to the DSEU to be passed to the spacecraft data system on a regular basis. High-speed time domain data for each sensor is collected in parallel with the scan data. The high-speed time domain data, "burst data", is stored into a 1-second deep circular buffer. The burst data can be commanded to be packetized and sent to the spacecraft. If enabled, a transient event algorithm will determine when a major event has occurred, packetize the time domain data, and send it to the DSEU.

Transient Event Detection

From ground tests we determined that engine starts, recycles, and grid arcs produce large E and B field

transients. Figures 5 and 6 illustrate the ion engine noise as sensed by the test monopole antenna and the flight-like plasma wave antenna. These measurements were performed in the "CT36" ground test in a JPL vacuum chamber. Notice the large spikes in the data; they are the results of an engine recycle. The surrounding signal is nominal engine noise. The spikes were at least five times greater than the typical engine noise. The duration of the event is usually less than one tenth of a second. A relatively simple algorithm for determining the presence of a transient was developed. The absolute values of the PWA and SC0 time domain signals are compared to a transient trigger level. If the signal exceeds the trigger level, the transient packaging process is initiated for the PWA, SC0 and FGM time domain data. The transient detection algorithm is performed twice for each 50 microsecond sample period, once on the PWA sample and once on the SC0 sample. Either one or both transient event detectors can be enabled or disabled.



5. RESULTS IN SPACE

Both the DSEU and FMP have successfully met their goals. In spite of the science search coil demise and the limited range of the Langmur probes, the NDP has collected much more than has been expected, both in data volume and in the different types of signals and phenomena. The FMP transient detection detects hydrazine thruster firings and Ion engine starts, restarts, and arcs. It detects Ion engine gimbal motor operation. It detects particle hits on the spacecraft. We have a lot of interesting time domain and scan data that we have not had the time to determine the exact cause or source.

An interesting little known fact is that hydrazine thrusters produce large spiked E and B field signals, generating noise, when they are fired. In fact, on DS1 the hydrazine thrusters noise spike is larger than the Ion engine operation noise and its transients. DS1 utilizes hydrazine thrusters for attitude control, which results in many thruster firings per day. In fact the transient detection has to be turned off for most of the

time so it wouldn't fill the data buffers and downlink capabilities. The FMP even detected a thruster firing that was not commanded. Speculation is that a high energy particle induced an SEU in the thruster command electronics causing the unintended activation of a thruster.

Following are examples of PWA and SC0 time domain data for different signal sources on the spacecraft.

Figures 7 through 14 are graphical representations of flight burst data. The transient detection algorithm detected and captured the burst event. The plots are 20,000 samples at 50-usec per sample. The left-hand side of the graph is time t0, or the first sample, proceeding right to sample 20,000

Ion Engine Start

Figures 7 and 8 show the start-up spike of the ion engine at the sample 10,000 on both the PWA and the SC0. The noise signal after the PWA spike is typical ion engine noise as sensed by the PWA.

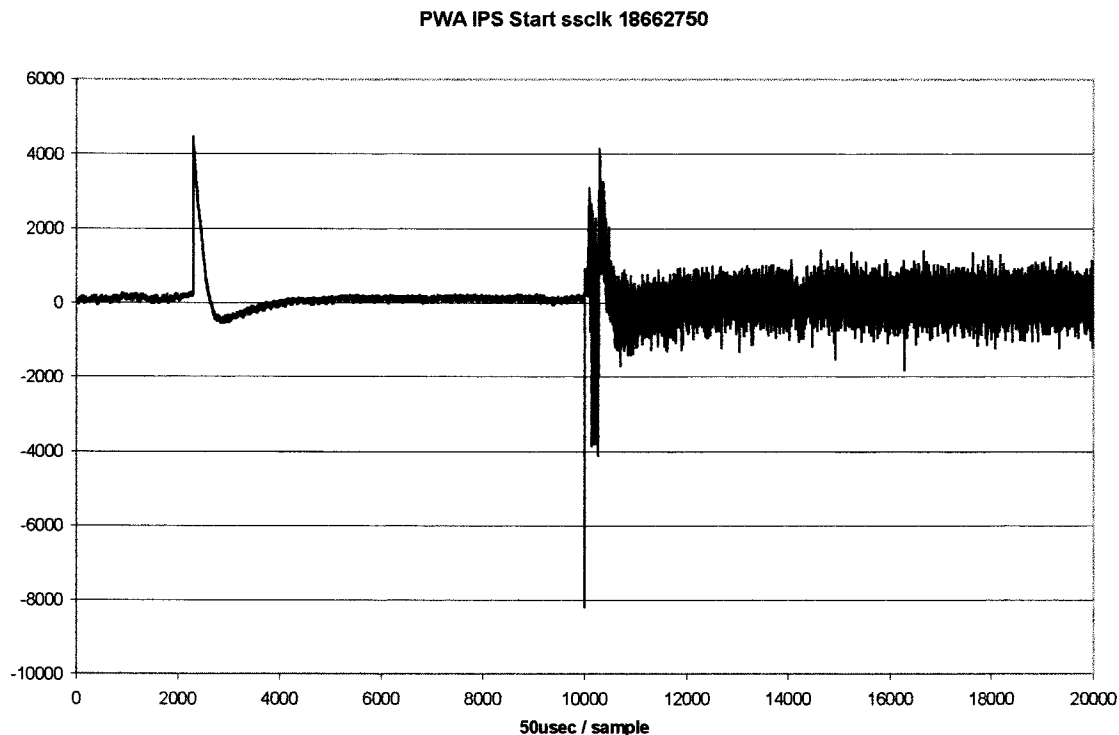


Figure 7. Plasma Wave Antenna IPS Start

SC0 IPS Start scik 18667250

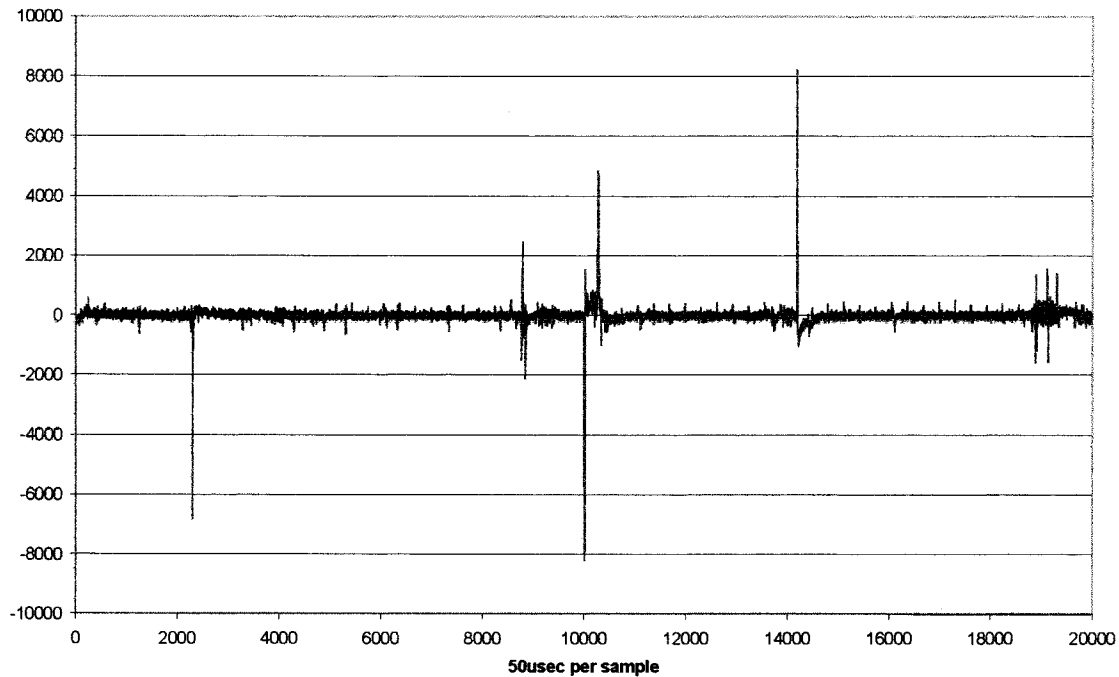


Figure 8. Search Coil (SC0) IPS Start

Ion Engine Recycle

Figures 9 and 10 show an ion engine recycle. The engine is on at the start of the left side of the graph. The engine extinguishes at data sample 900 and

restarts at data point 10,000. In the SC0 plot, the signal starting approximately at the 4000 sample and continuing to approximately sample 19,000 is mostly the engine gimbal actuator fields, not the ion engine.

PWA Engine Recycle scik 12410534

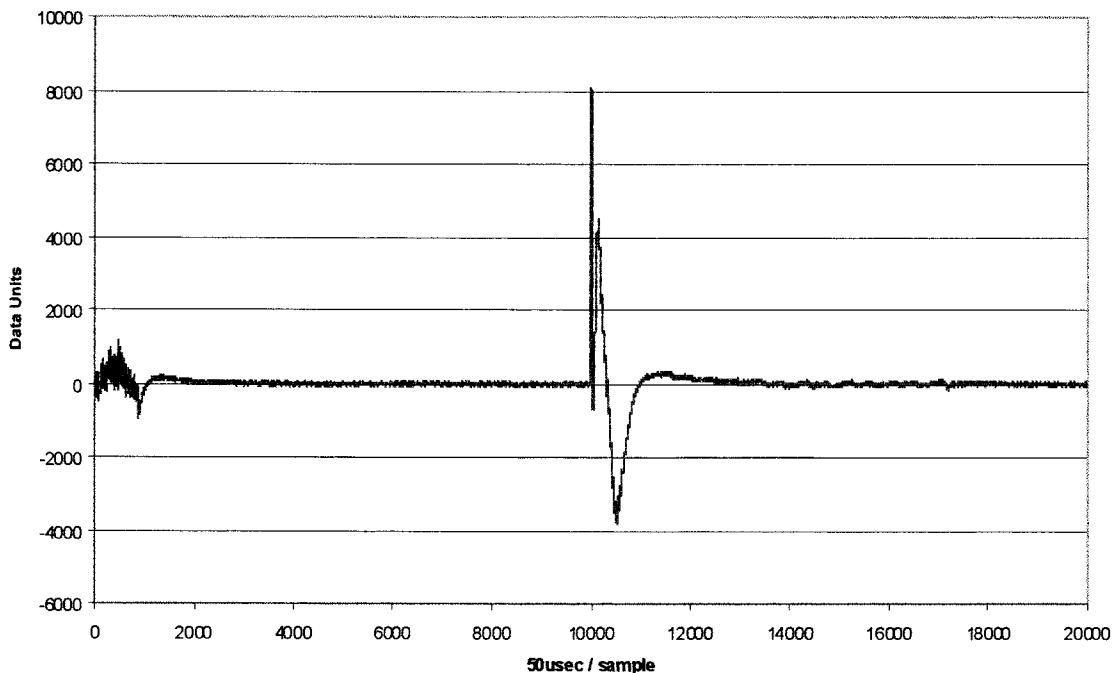


Figure 9. Plasma Antenna Recycle Event (scik = spacecraft clock time from start of mission)

SC0 Engine Recycle sclk 12410534

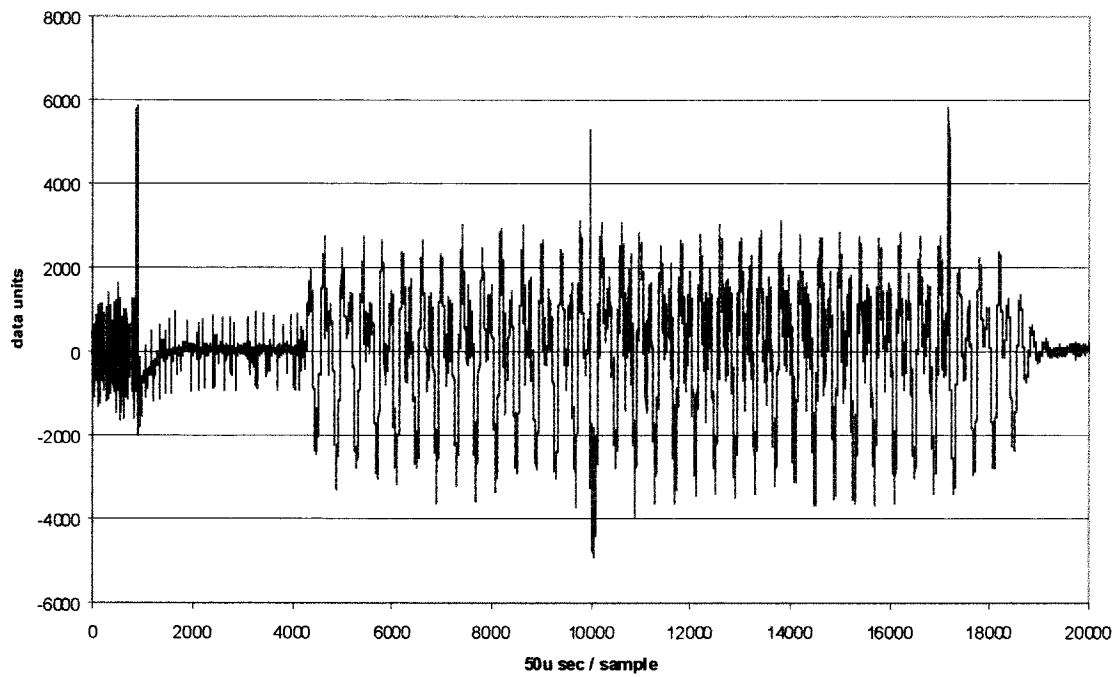


Figure 10. Search Coil (SC0) Recycle Event

Hydrazine thruster firing

Figures 11 and 12 show the noise spikes of the hydrazine thruster pair X2 and X4. This example is

of a short thrust duration. Some thruster firings have been observed to be a quarter of a second in duration.

PWA Hydrazine Thrusters X2, X4 sclk 11467714

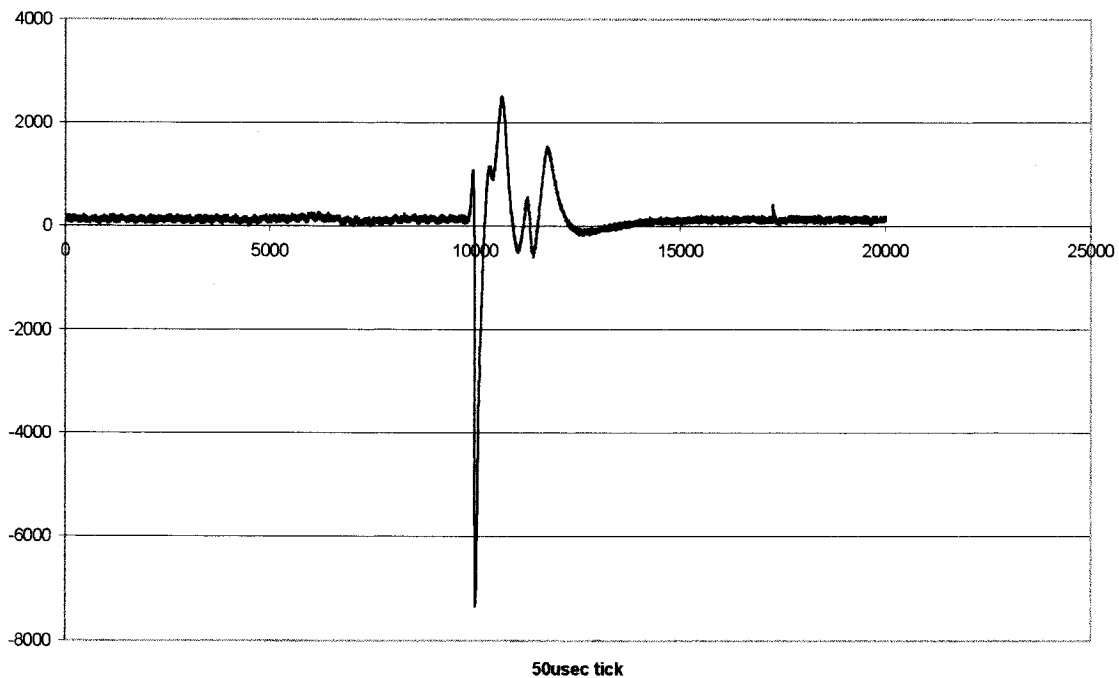


Figure 11. Plasma Wave Antenna Event Associated with Firing of Hydrazine Thrusters X2 and X4

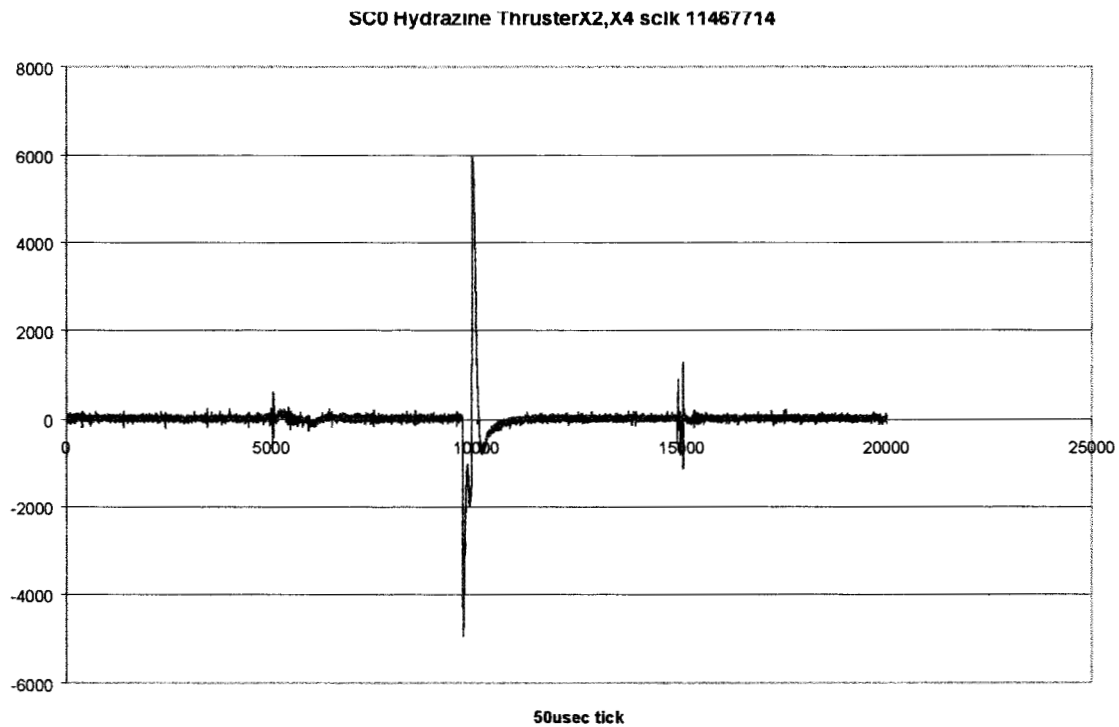


Figure 12. Search Coil (SC0) Event Associated with Firing of Hydrazine Thrusters X2 and X4

Particle Impact

Figures 13 and 14 show the signal generated by a

particle hit on the spacecraft. Notice there is no magnetic field in SC0.

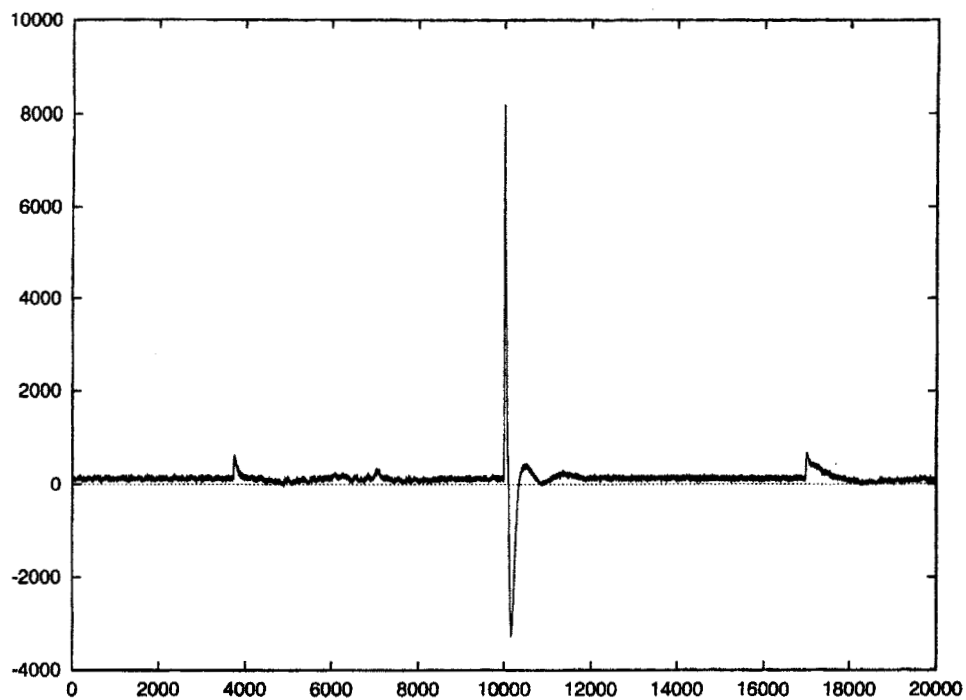


Figure 13. Plasma Wave Antenna Event Associated with Particle Impact

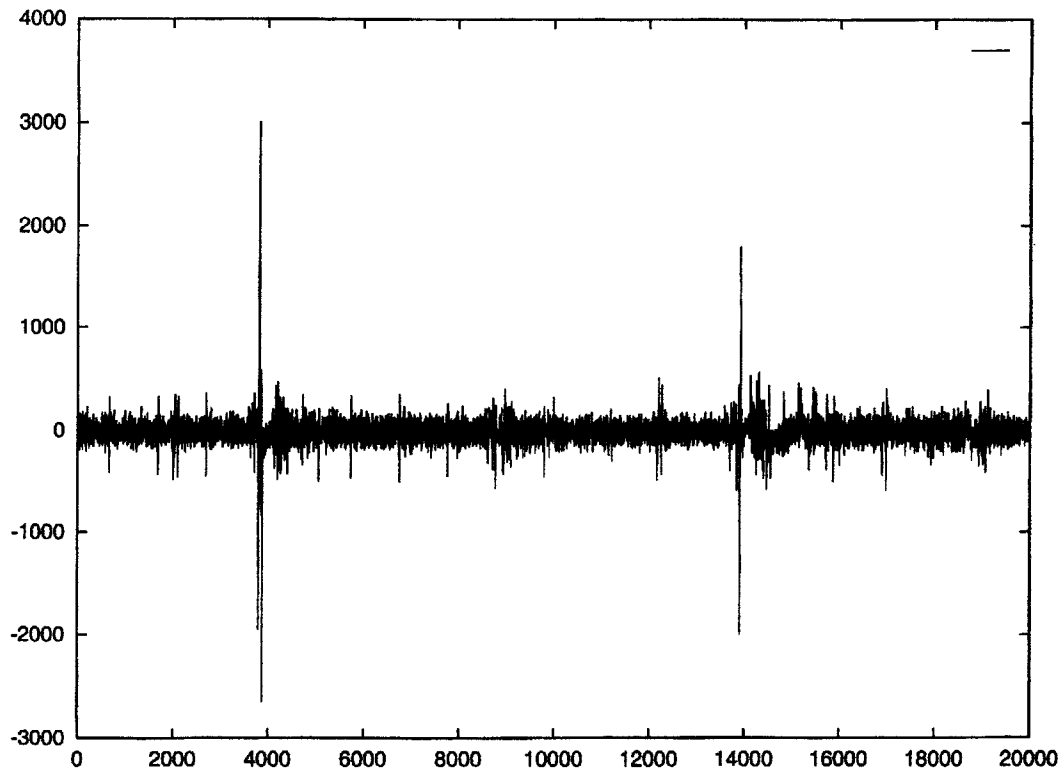


Figure 14. Search Coil (SC0) Event Associated with Particle Impact

Spectrometer Data

Figures 15 and 16 show the plasma wave spectrometer data during the ion engine operation. They show the engine at thrust level two. It shows the increase in noise level and increase into lower frequency noise for the period that the engine is pressurizing up for throttle level three. Once the engine is pressurized for thrust level three, the electrical parameters for the engine change to level three, and the noise reduces in level and frequency width. Note, as one would expect, the level-three noise is a little higher than level two. Figure 15 is a topographic representation of the spectrometer data.

Figure 16 is a three-dimensional view of the same data.

Figure 17 shows a larger increase in noise as it changes to level four thrust. Notice though that the pressurization is not as noisy.

Figure 18 is a surprising result of thruster level change. This chart shows the transition from thrust level zero (ML6) to thrust level one (ML13). Notice the noise reduces dramatically. Work is in progress to characterize the cause of this reaction. It is believed that the density of the charge exchange ions is a major cause of this phenomenon.

DS1 IAT2 PWL: TH2 to TH3
1999-148/19:50:54 to 1999-148/20:05:00

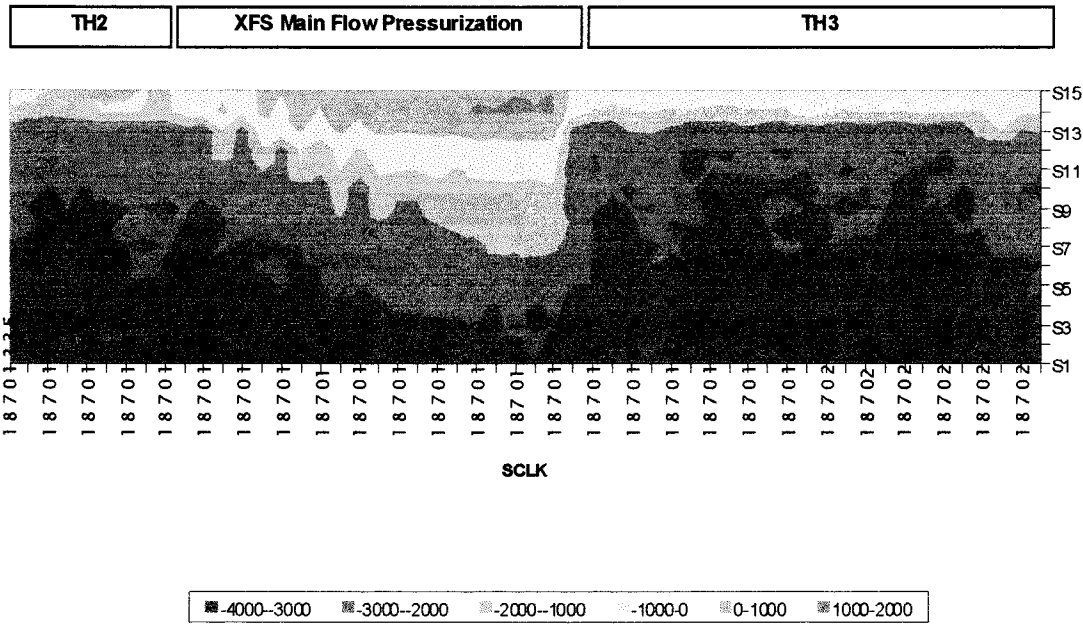


Figure 15.

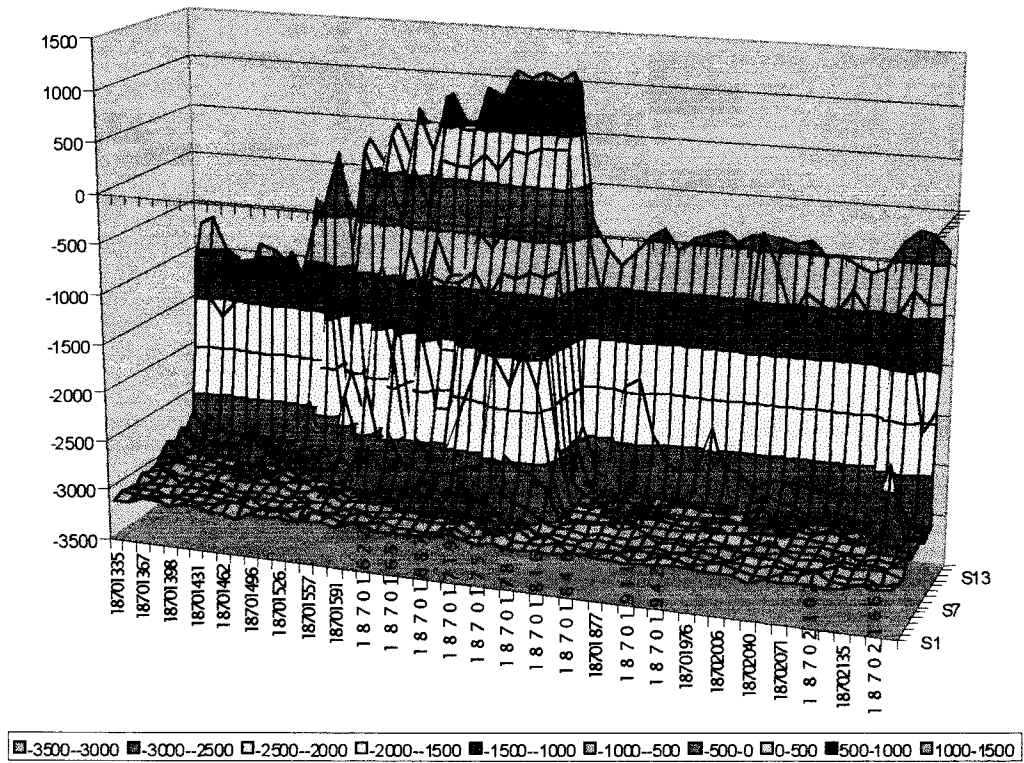


Figure 16.

DS1 IAT2 PWL: TH3 to TH4
1999-148/21:50:45 to 1999-148/22:02:44

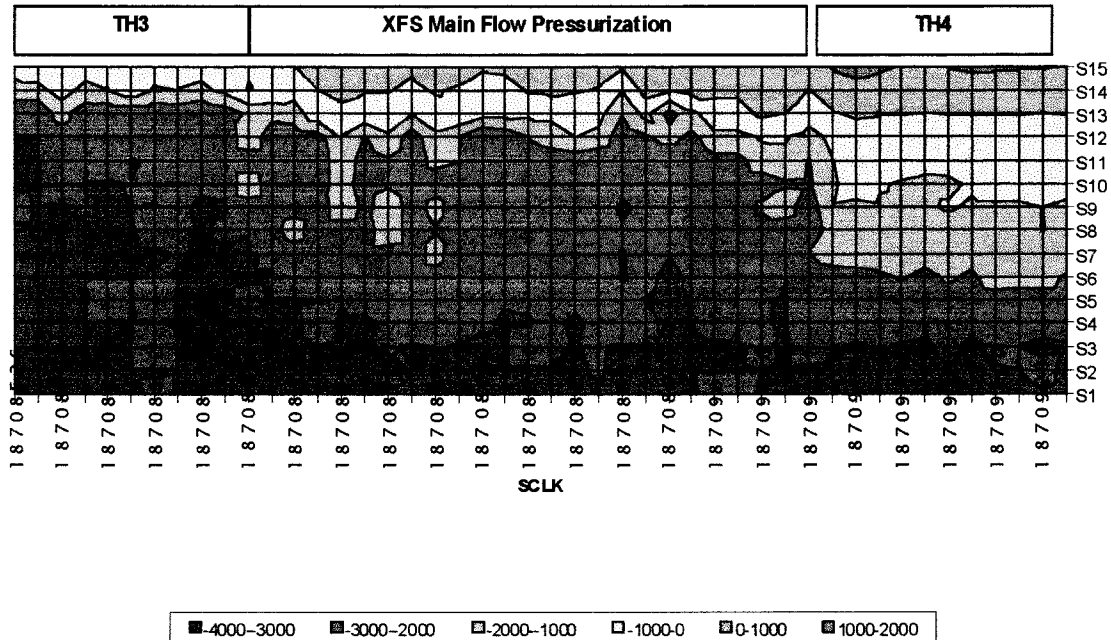
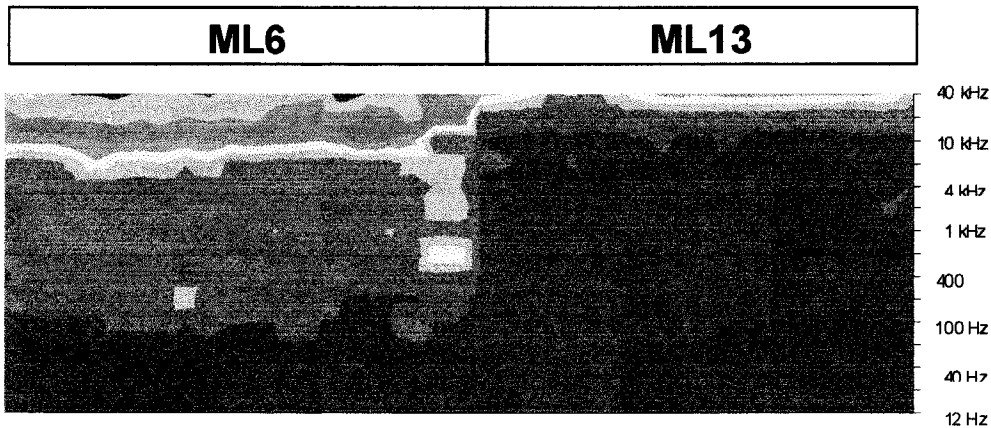


Figure 17.

DS1 IAT2: NDP Plasma Wave Low-Frequency Spectrometer
1999-148/16:47:10 to 1999-148/16:58:05
Transition from IPS ML6 to IPS ML13



Plasma noise decrease for transition to higher thrust level
 ML13 is more efficient in Xe propellant utilization than ML6
 Excess Xe neutral gas produces more charge exchange plasma
 Charge exchange plasma is conducting medium for electrical noise

Figure 18.

6. CONCLUSION

DS1 is the first in-depth investigation of an ion propulsion systems interaction with an interplanetary spacecraft in flight. The NDP has succeeded in capturing characteristic data on the different phases and thrust levels of the IPS.

From a spacecraft systems engineering perspective, Ion propulsion does not produce electromagnetic or electrostatic noise beyond that of other typical spacecraft subsystems. Though the Ion engine produces noise continuously while it's on and the spacecraft noises are typically transitory.

The NSTAR Ion engines noise can be bounded by the following:

E-field
0 to 10 MHz 0.01 V/m
10 MHz to 30 MHz and beyond -3
dB/decade starting at 0.01 V/m

B-field
0 to 10 MHz

E & B field Transients
Less than 10 V/m for less than 0.1 second

DS1 gimbals and solar array motors noise can be bounded by:

E-field
No E-field observed
B-field
Less than 40 micro Tesla, 0 to 10
kHz range

DS1 spacecraft particle hits have been:

E-field
10 V/m for less than 0.1 sec
B-field
No B-field signal observed

From the spectrometer data we hope to be able to measure the efficiency of the engine and to provide data to help produce better engine parameter tables which will provide a more efficient and longer lasting engine.

7. REFERENCES

- [1] M. P. Raymen, P. Varghese, D. H. Lehman, L. L. Livesay, Results from the Deep Space 1 Technology Validation Mission IAA-99-IAA.11.2.01, 50th Int. Astronautical Congress 4-8 Oct. 1999, Amsterdam, the Netherlands.
- [2] Report on the NASA/USAF Workshop on Environmental Diagnostics for ELITE/STAR, October 20-21, 19993 (JPL internal document), Jet Propulsion Laboratory, Pasadena, CA, March 1, 1994.
- [3] Industry User's and Manufacturer's Survey, JPL IOM 355-1-93 (JPL internal document), Jet Propulsion Laboratory, Pasadena, CA, Dec. 7, 1993.
- [4] R. Kakuda, J. Sercel, W. Lee, J. Riehl, NSTAR User Performance Needs Report, JPL D-12672 (JPL internal document), Jet Propulsion Laboratory, Pasadena, CA, May 1995.

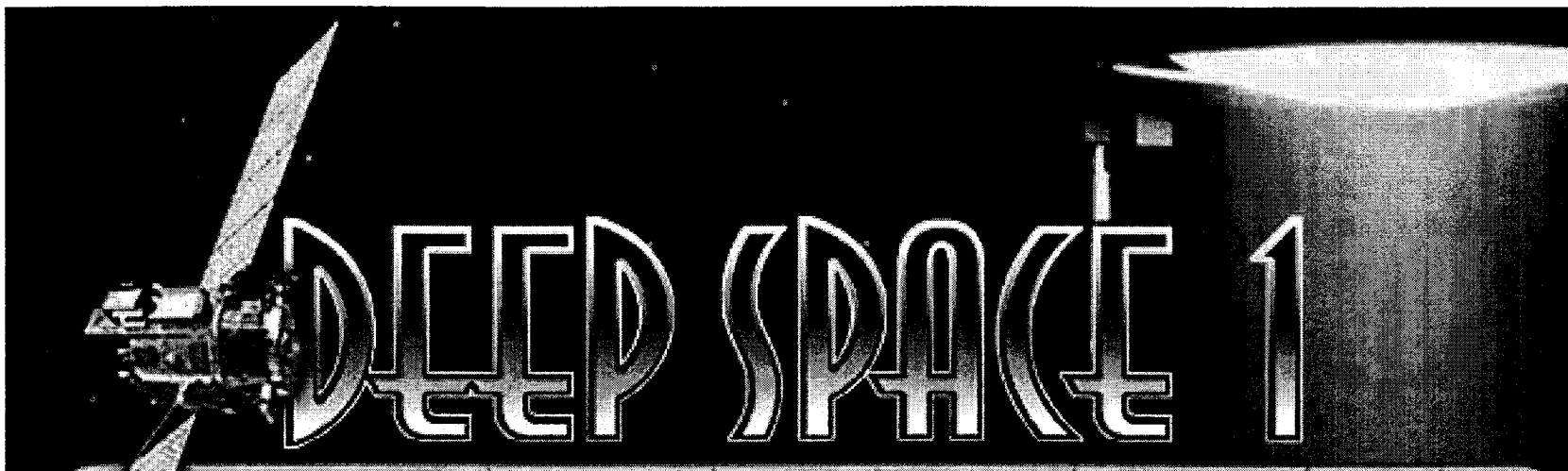
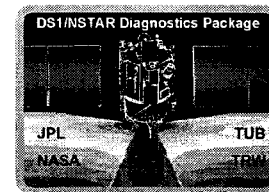
8. ACKNOWLEDGMENTS

The research described in this paper was carried out by the Jet Propulsion Laboratory, California Institute of Technology, under a contract with the National Aeronautics and Space Administration. It also includes several critical electronic components that were developed by TRW using TRW internal research and development funding. Finally, the Institute for Geophysical and Meteorology of the Technical University of Braunschweig provided the Flux Gate Magnetometers and their signal conditioning board, utilizing their own funding.



NSTAR Diagnostic Package Architecture and Deep Space One Spacecraft Event Detection

CL 99-1936



Michael D Henry, *et al*
Jet Propulsion Laboratory
California Institute of Technology
michael.d.henry@jpl.nasa.gov
(818)354-1553

IEEE Aerospace Conference
Big Sky MT
March 18-25, 2000



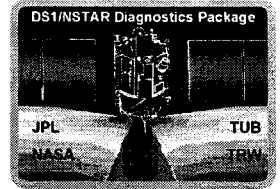
Goal for IDS



- **Understand the local environment on a spacecraft utilizing an Ion Propulsion Subsystem (IPS)**
 - What is the nature of the local plasma environment?
 - What is the IPS contamination environment?
 - Are there EMI/EMC concerns?
 - Are IPS DC-magnetic fields compatible with science measurement requirements?



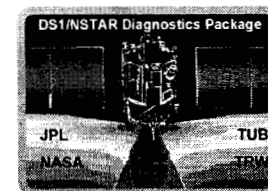
IDS Team Members



- **JPL**
 - Principle Investigator: David E Brinza
 - FMP: M. Henry, A. Mactutis, K. McCarty, J. Rademacher, T. vanZandt, K. Leschly, B. T. Tsurutani
 - Modeling: J. J. Wang
- **Technical University of Braunschweig**
 - FGM: G. Musmann, I. Richter, C. Othmer, K-H. Glassmeier
- **TRW**
 - PWS: S. Moses, R. Johnson
- **Maxwell Technologies**
 - Modeling: I. Katz, V. Davis, B. Gardner
- **Physical Sciences, Inc.**
 - DSEU (SAMMES heritage: BMDO) and Calorimeters: E. Lund, P. Joshi, M. Hinds, B. D. Green



IDS Flight Hardware

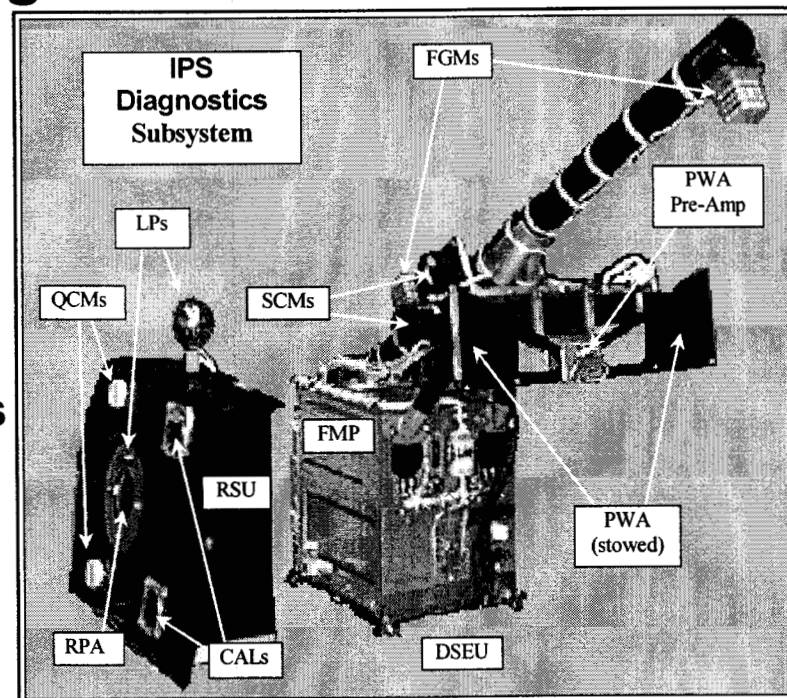


- **IDS is a compact, highly-integrated sensor suite**

- Mass: 8 kg
- Power: 21W , 7W (standby)
- Spacecraft Interfaces:
 - 28 VDC (± 6 VDC), MIL-STD-1553B

- **IDS samples continuously**

- RSU sensors at 2 second intervals
- FMP scans at 16 second intervals
- Waveform transient recording
 - PWA, SC at 20 kHz, 1 second
 - FGMs at 20 Hz, 55 seconds



Remote Sensors Unit (RSU):

Plasma: 2 Langmuir Probes(LPs), Retarding Potential Analyzer (RPA)

Contamination: 2 Quartz Crystal Microbalances (QCMs), 2 Calorimeters (CALs)

Diagnostic Sensors Electronics Unit/Fields Measurement Processor (DSEU/FMP):

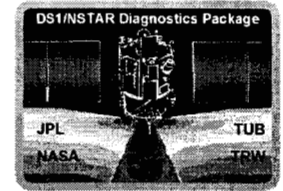
Electrostatic Fields: 2-m dipole Plasma Wave Antenna (PWA) with pre-amplifier

Electromagnetic Waves: 2 Search Coil Magnetometers (SCMs); 1 failed before launch

DC Magnetic Fields: 2 ea. 3-axis Flux-Gate Magnetometers (FGMs)



IDS Sensor Performance



- IDS sensors were calibrated over the operating temperature range (-25°C to +55°C)
- Measurement capabilities summarized below

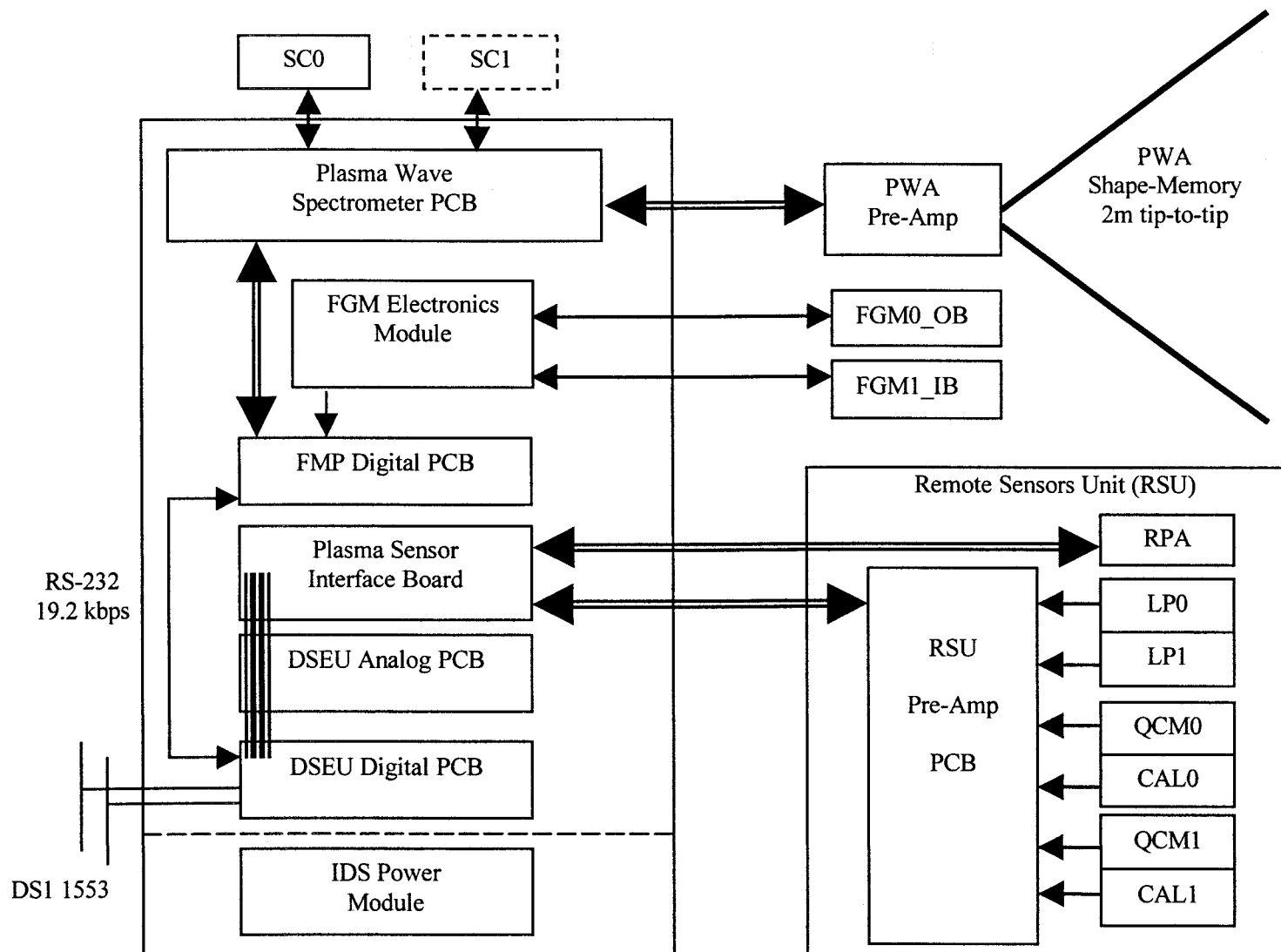
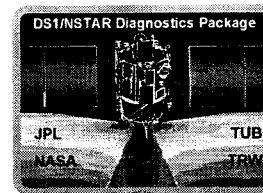
Sensor	Measurement	Range	Resolution
QCMs	Mass/area	0 to 500 $\mu\text{g}/\text{cm}^2$	0.01 $\mu\text{g}/\text{cm}^2$
CALs	Solar Absorptance (α) Hemi. Emittance (ε)	$\alpha = 0.08$ (BOL) to 0.99 $\varepsilon = 0.05$ to 0.85 (BOL)	$\Delta\alpha = 0.01$ $\Delta\varepsilon = 0.01$
LPs	Probe Current Probe Voltage	$I = -0.4$ to 40 mA $V = -11$ to +11 VDC	1% 0.1V
RPA	Current (Gain Select) Grid Bias Voltage	$I = 0.01, 1, 10, 100\mu\text{A}$ $V = 0$ to +100 VDC	1% 0.4V
PWA	E-field (Adjust. Gain) 24 Freq. Channels *	50 to 160 dB $\mu\text{V}/\text{m}$ 10 Hz to 30 MHz (4/decade)*	± 3 dB $\mu\text{V}/\text{m}$ $\pm 40\%$ (-3dB)**
SCM	B-field (Adjust. Gain) 16 Freq. Channels *	80 to 160 dBpT 10 Hz to 100 kHz (4/decade)*	± 3 dBpT $\pm 40\%$ (-3dB)**
FGMs	Magnetic Field Vector **	$\pm 25,000$ nT	0.5 nT

* Typical band separation

** Typical Bandwidth

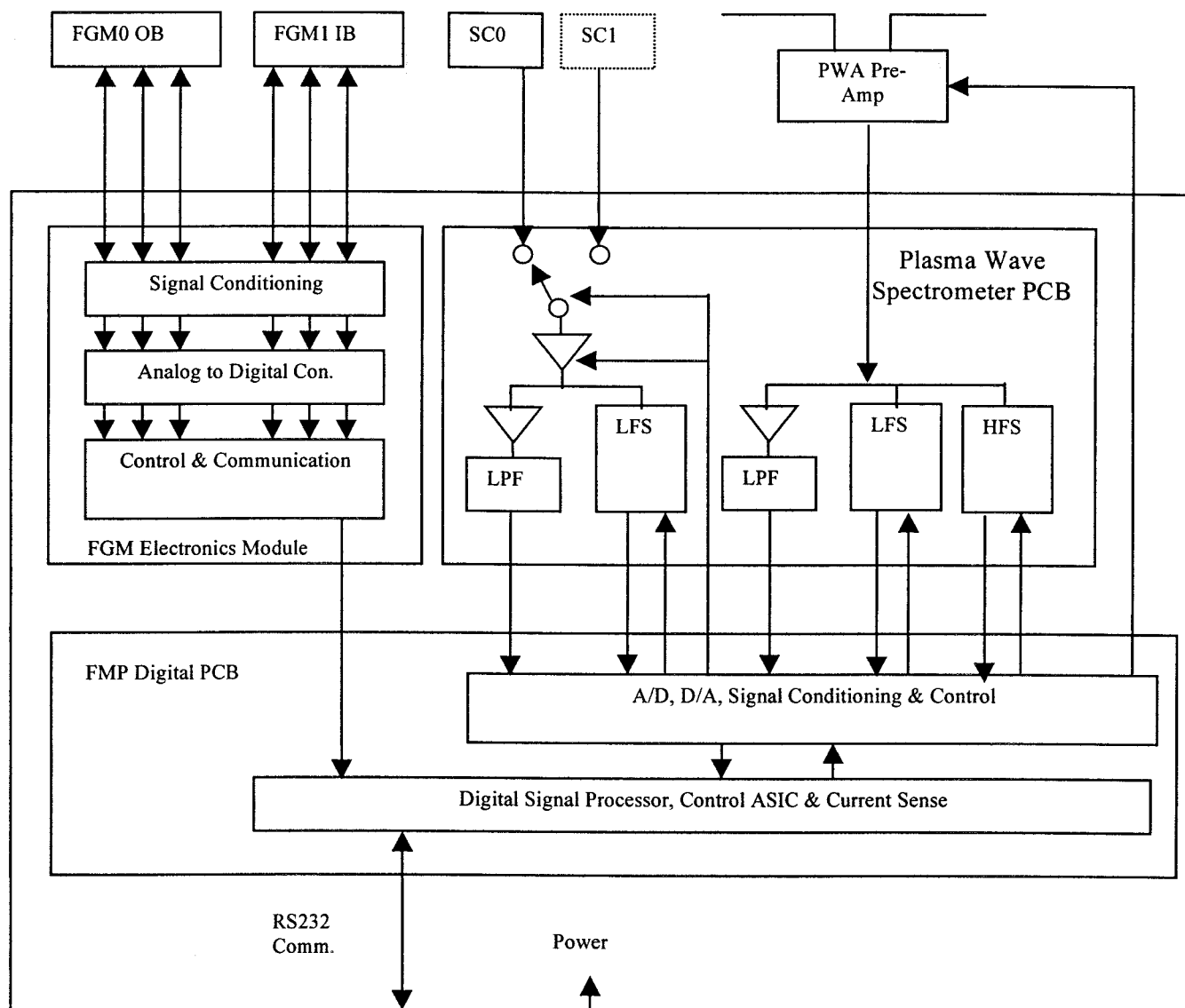
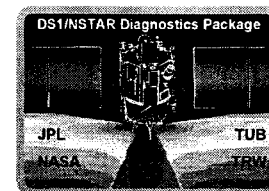


NSTAR Diagnostic Package Block Diagram



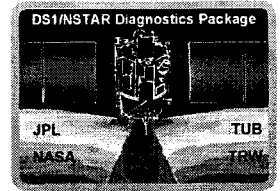


Fields Measurement Processor Block Diagram

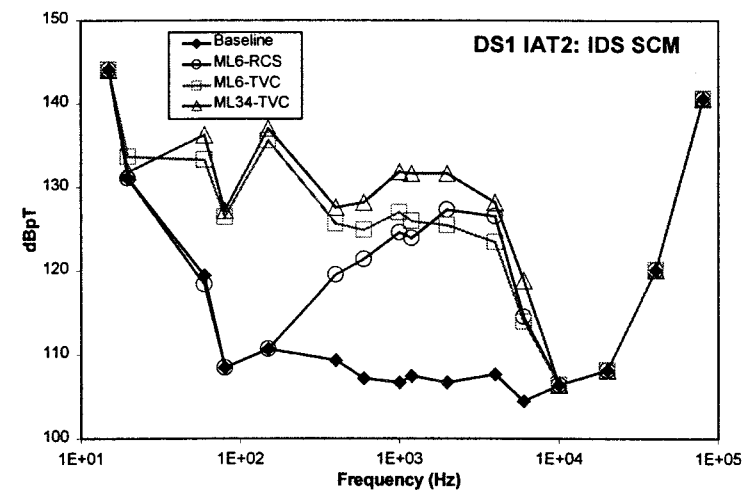
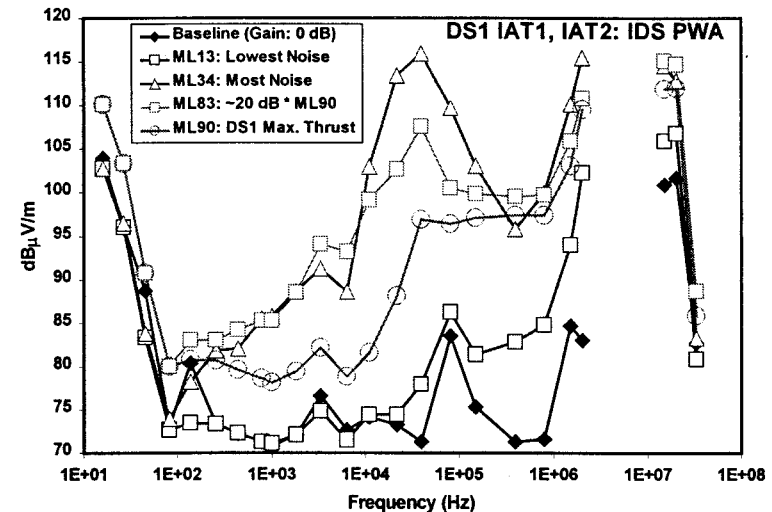




IDS Plasma Wave Measurements

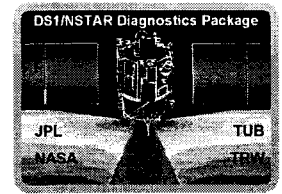


- **Plasma Waves**
 - $<120 \text{ dB}_\mu\text{V}$ maximum
 - IPS ignition or recycles produce peak amplitude signals comparable to hydrazine thruster firings ($<140 \text{ dB}_\mu\text{V/m}$)
- **EMI (AC B-field)**
 - IPS produces EM noise ($<140 \text{ dBpT}$ @ 2 kHz)
 - Ion engine gimbal motors for TVC produce similar EMI levels at 100 Hz
 - IPS has no impact on telecommunications link

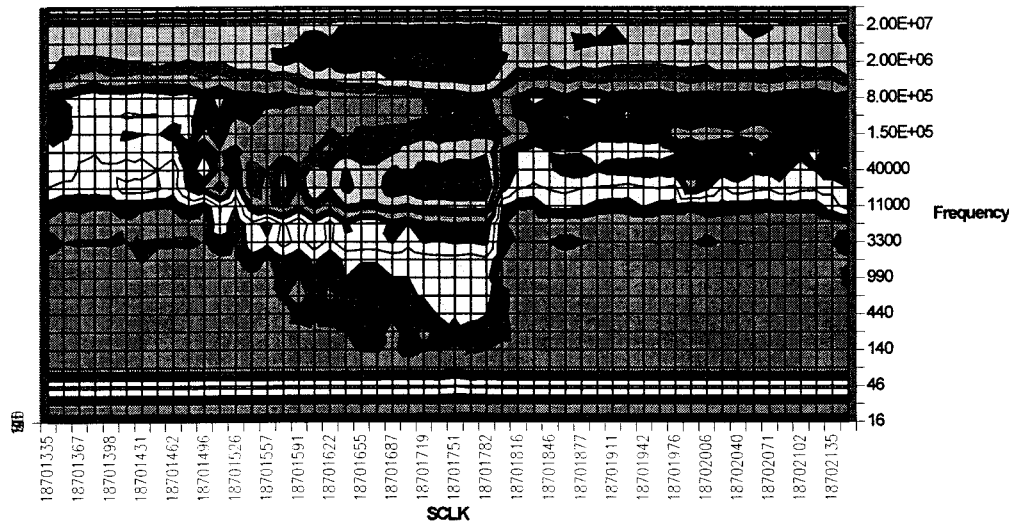




Expected Thrust Level Transitions

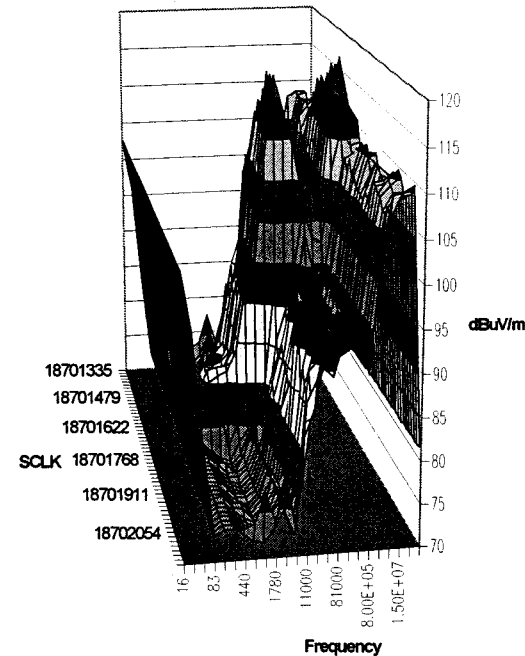


PWS IAT2 M20 to M27 Transition



dBV/m ■ 70-75 ■ 75-80 ■ 80-85 ■ 85-90 ■ 90-95 ■ 95-100 ■ 100-105 ■ 105-110 ■ 110-115 ■ 115-120

PWS IAT2 ML20 to ML27



■ 70-75 ■ 75-80 ■ 80-85 ■ 85-90 ■ 90-95 ■ 95-100 ■ 100-105 ■ 105-110 ■ 110-115 ■ 115-120

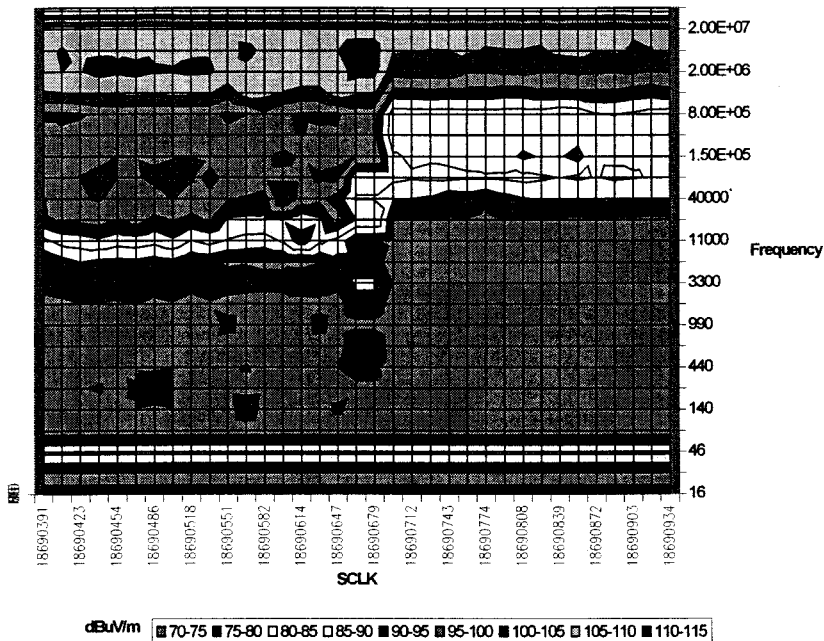
- Noise level ML 20 is 105dBuV/m at 200kHz
- Noise increases as flow is increased in preparation for transition to ML 27, peak ~ 118dBuV/m
- Noise settles to a slightly larger level, 106dBuV/m at 200kHz



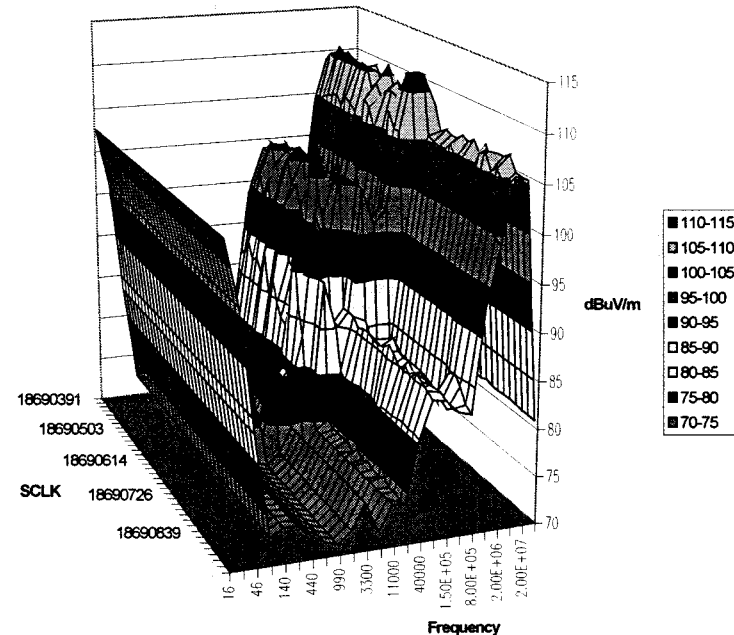
Interesting Thrust Level Transitions



PWS IAT2 ML6 to ML13
iat2_pws_plan_views.xls



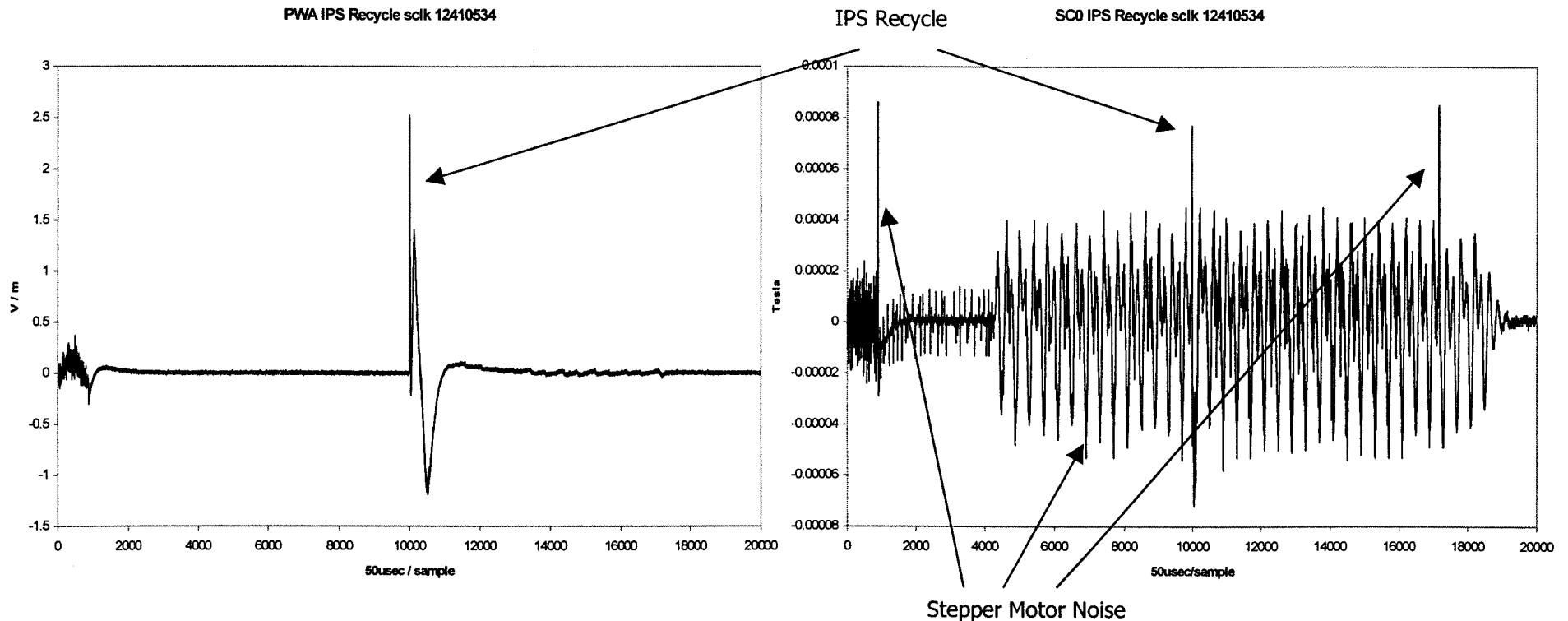
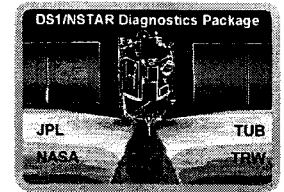
PWS IAT2 ML6 to ML13



- An increase in thrust level doesn't always produce an increase in noise
 - Mission Level 6 is much noisier than Mission Level 13



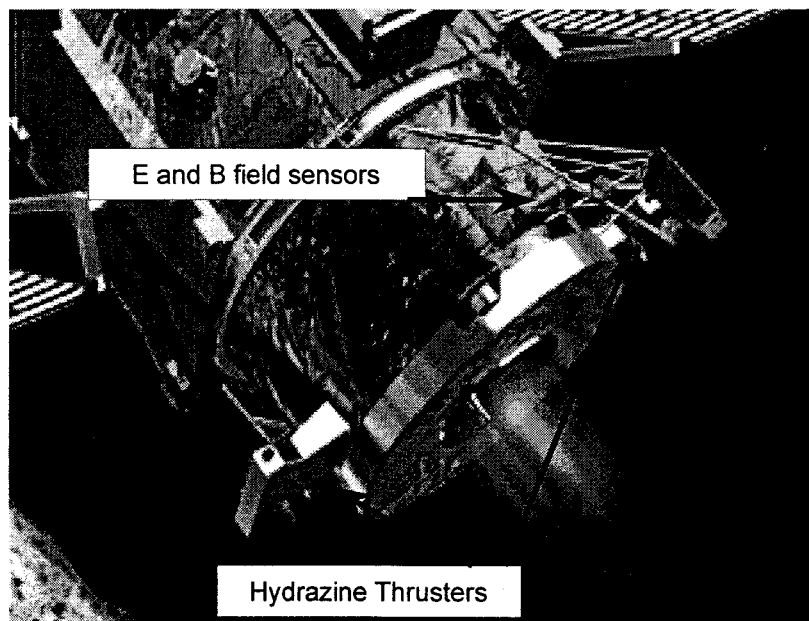
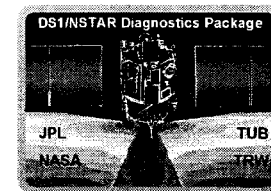
Typical IPS Recycle



- E field peak ~ 2.5 V/m
- B field peak ~ 80 uTesla
 - Notice stepper motor noise is of the same level of the IPS recycle in B field

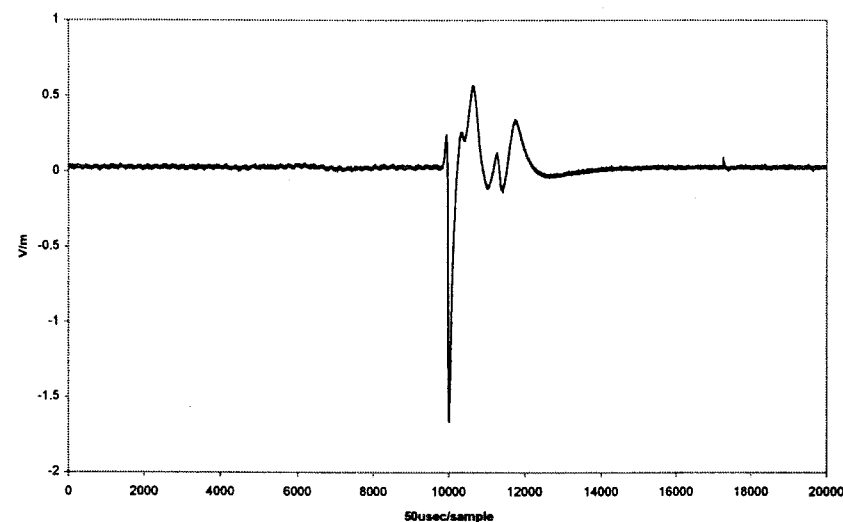


Typical Hydrazine thruster E and B field signature

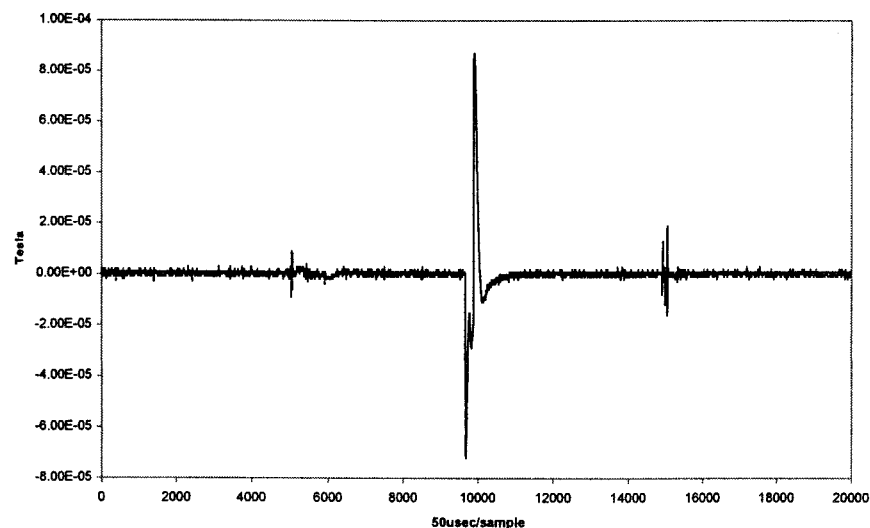


- E field ~ 2 Volts per Meter
- B field 0.8 micro Tesla

PWA Hydrazine Thrusters X2, X4 sclk 11467714

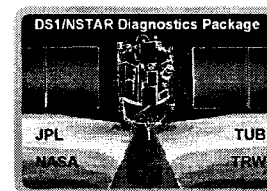


SC0 Hydrazine Thruster X2, X4 sclk 11467714



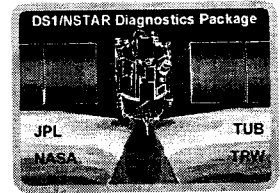


Back Up Slides





IDS Conclusions



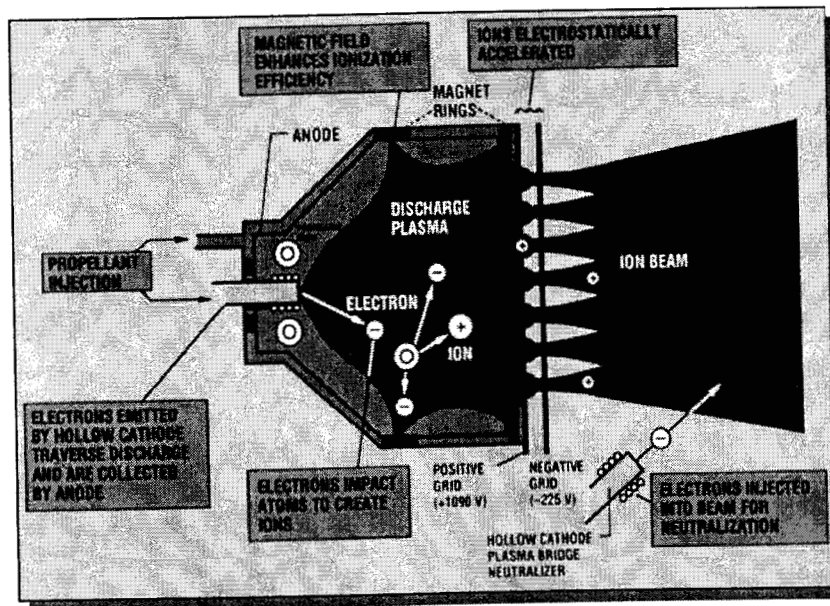
- **IPS local environment well-characterized**
 - **CEX plasma affects DS1 chassis potential**
 - CEX ions surround DS1, substantial ion flux for particle spectrometers, solar wind protons unaffected
 - **Local line-of-sight contamination rates are substantial**
 - Non-line-of-sight contamination rates are significantly lower
 - **Plasma waves are produced by IPS**
 - Peak amplitudes are equivalent to other sources on DS1 (hydrazine thruster firings, IPS gimbal motor operations)
- **Further investigations in progress**
 - Effects of sun-orientation on chassis potential
 - Long-term contamination rates vs IPS ML
 - Plasma wave noise dependence on IPS operating conditions (Why is ML90 much quieter than ML83?)



IPS Operation and Charge Exchange Xenon Ions



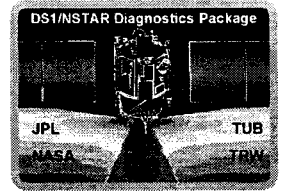
- IPS produces beam and cold, dense plasma flow
 - IPS ionizes 80% to 90% of xenon in discharge chamber
 - Fast beam ion strips electron from slow thermal xenon atom
$$\text{Xe}^+_{\text{beam}} + \text{Xe}^0_{\text{thermal}} \longrightarrow \text{Xe}^0_{\text{beam}} + \text{Xe}^+_{\text{CEX}}$$
 - “Charge-exchange xenon” (CEX) ions driven by local E-fields



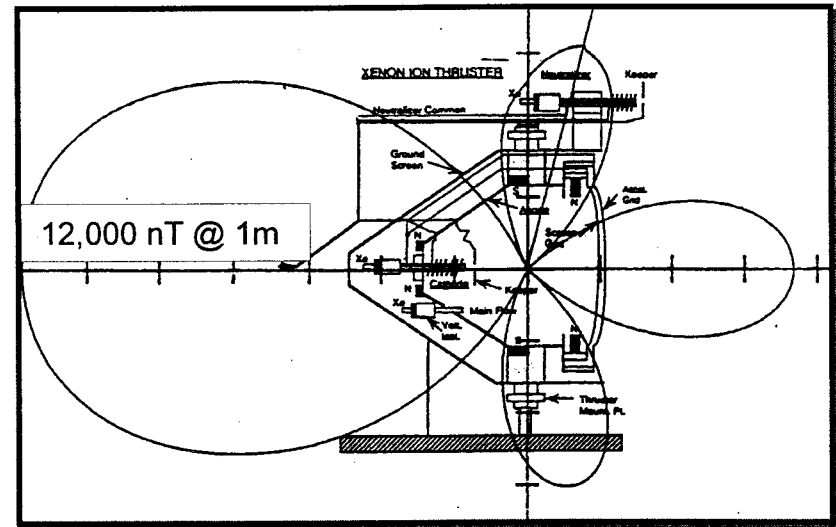
- CEX ions affect these environmental factors
 - DS1 chassis potential
 - IPS contamination
 - Plasma wave noise



IPS DC Magnetic Field



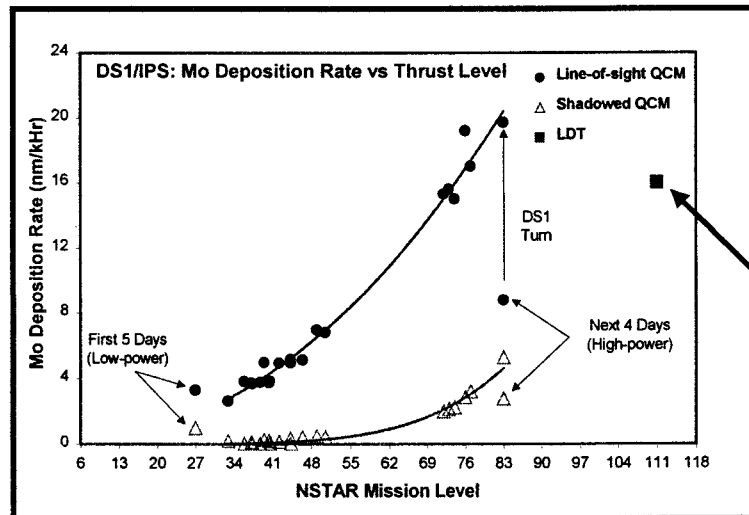
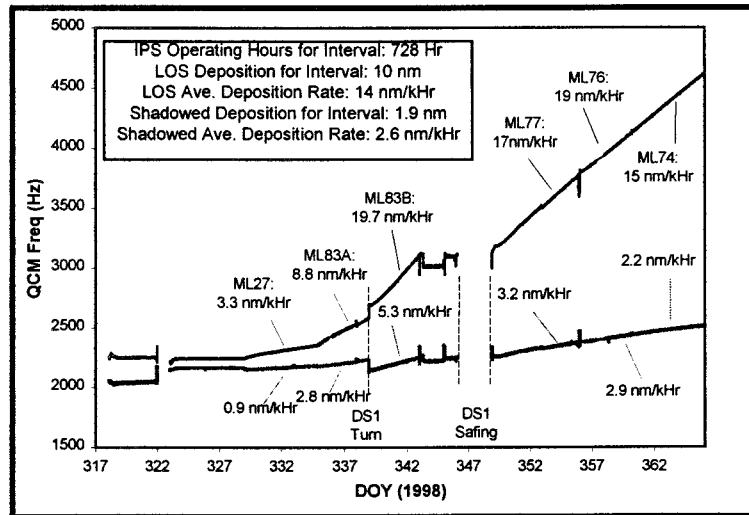
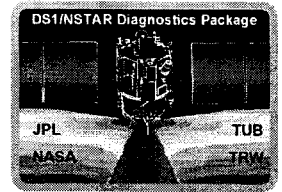
- **$\text{Sm}_2\text{Co}_{17}$ magnet rings within IPS thruster**
 - “Ring-cusp” geometry to improve IPS xenon ionization efficiency
 - External fields $\sim 10,000$ nT at 1 meter distance
 - Temperature-dependence characterized in flight



- **Magnetic field stability and science measurements**
 - Temperature-corrected DC fields stable within 5 nT after 1 year operation ($< 0.1\%$ change since launch)
 - No long-term degradation trend for magnetic fields obvious
 - Short-term magnetic field stability allows measurement of fluctuations (> 1 nT) of external B-fields



IDS Contamination Measurements



- Mo deposition readily detected by QCMs
 - Line-of-sight deposition shown in figure to left is >5x shadowed sensor
 - Sun-orientation effect on deposition for ML83A/B (DOY 98-335 to 98-344)
- Mo deposition rate vs IPS Mission Level (ML)
 - Correlates with current collected by outer grid
 - Highest IPS levels only at beginning of mission
 - Ground test (LDT) result is for maximum IPS ML